ARL-TR-7368 ● AUG 2015

US Army Research Laboratory

Investigation of Surface Preparations to Enhance Photon Doppler Velocimetry Measurements

by Michael B Zellner, Chester A Benjamin, Robert W Borys Sr, Ronald Cantrell, Kennith W Dudeck, Nathan J Sturgill, and Corey E Yonce

NOTICES

Disclaimers

The findings in this report are not to be construed as an official Department of the Army position unless so designated by other authorized documents.

Citation of manufacturer's or trade names does not constitute an official endorsement or approval of the use thereof.

Destroy this report when it is no longer needed. Do not return it to the originator.

ARL-TR-7368 ● AUG 2015

US Army Research Laboratory

Investigation of Surface Preparations to Enhance Photon Doppler Velocimetry Measurements

by Michael B Zellner, Chester A Benjamin, Robert W Borys Sr, Ronald Cantrell, Kennith W Dudeck, Nathan J Sturgill, and Corey E Yonce

Weapons and Materials Research Directorate, ARL

REPORT DOCUMENTATION PAGE

Form Approved
OMB No. 0704-0188

1. REPORT DATE *(DD-MM-YYYY)*	2. REPORT TYPE	3. DATES COVERED (From - To)
August 2015	Final	October 2015–September 2015

4. TITLE AND SUBTITLE
Investigation of Surface Preparations to Enhance Photon Doppler Velocimetry Measurements

5a. CONTRACT NUMBER

5b. GRANT NUMBER

5c. PROGRAM ELEMENT NUMBER

6. AUTHOR(S)
Michael B Zellner, Chester A Benjamin, Robert W Borys Sr, Ronald Cantrell, Kennith W Dudeck, Nathan J Sturgill, and Corey E Yonce

5d. PROJECT NUMBER
AH80

5e. TASK NUMBER

5f. WORK UNIT NUMBER

7. PERFORMING ORGANIZATION NAME(S) AND ADDRESS(ES)
US Army Research Laboratory
ATTN: RDRL-WMP-D
Aberdeen Proving Ground, MD 21005-5069

8. PERFORMING ORGANIZATION REPORT NUMBER
ARL-TR-7368

9. SPONSORING/MONITORING AGENCY NAME(S) AND ADDRESS(ES)

10. SPONSOR/MONITOR'S ACRONYM(S)

11. SPONSOR/MONITOR'S REPORT NUMBER(S)

12. DISTRIBUTION/AVAILABILITY STATEMENT
Approved for public release; distribution is unlimited.

13. SUPPLEMENTARY NOTES

14. ABSTRACT
The work described in this report compiles empirical measurements of the intensity of 1.55-μm light reflected from numerous materials prepared with varying surface finishes over a range of incident and detection angles. The data are desired to construct a guide for conducting Photon Doppler Velocimetry measurements, which necessitates a prediction of the intensity of Doppler shifted light that will be reflected from a surface to optimize the measurement. It was found that the intensity of reflected light could be sufficiently explained using the law of reflection coupled with a coefficient of reflection that is specific to the material. It also provides a technique for empirically measuring the latter.

15. SUBJECT TERMS
photon doppler velocimetry, reflected light, law of reflection, coefficient of reflection

16. SECURITY CLASSIFICATION OF:			17. LIMITATION OF ABSTRACT	18. NUMBER OF PAGES	19a. NAME OF RESPONSIBLE PERSON
a. REPORT	b. ABSTRACT	c. THIS PAGE			Michael B Zellner
Unclassified	Unclassified	Unclassified	UU	72	19b. TELEPHONE NUMBER (Include area code) 410-306-2565

Contents

List of Figures

List of Tables

INTENTIONALLY LEFT BLANK.

1. Introduction

Photon Doppler Velocimetry (PDV) is an experimental technique that estimates the velocity with which a reflector is moving by examining the Doppler shift of light scattered from its surface.[1,2] The fundamental physics underpinning this technique are a direct extrapolation of those recognized by Christian Doppler in 1842.[3] Recently, academics studying within the field of shock physics recognized that the invent of fiber-based lasers, optical circulators, and fast digitizers allowed for one to make a compact system capable of measuring the Doppler shift from reflectors utilizing light within the infrared portion of the spectrum ($\lambda = 1.55$ μm).[1] These systems operate with subnanosecond temporal response and can measure velocities ranging from approximately zero to upwards of 10 mm/μs. Also, depending on the analysis method, it is not necessary to ensure coherence of the scattered light throughout the measurement. In a practical sense, this means that one can make measurements from many scattering centers, each with differing velocities, simultaneously, such as that which occurs when a small amount of particles are ejected from an accelerated free surface.

Deployment of these systems throughout Army research facilities is becoming very popular because of the technique's versatility and applicability to measure many velocities that the Army is interested in: floor accelerations due to an under-vehicle mine blast;[4] material deformations from a bullet impact;[5] maximum tip velocities of a jet formed from detonation of a shaped charge,[6] and so forth. The technique does pose limitations, such as only being capable of making a velocity measurement of a single point, but it is compatible with silicon detector based techniques such as optical photography or digital image correlation, which can provide full field-of-view. One limitation of the technique that this report aims to address is the capability to predict how much light will be scattered from the reflecting surface during a dynamic event. This is not a simplistic problem, as in some scenarios the surface may undergo a shock induced phase change or a chemical reaction. In these cases, the intensity of light being scattered is dependent on the changes that the material index of refraction undergoes, which may or may not be predictable. However, when accelerations of the reflecting surface are insufficient to cause the surface to yield across its entirety, it is possible to provide general rules guided by empirical measurements, to suggest what intensity of light will be scattered at varying angles.

Figure 1 depicts a schematic of a PDV system, where f_0 represents a path in which the light has the original frequency, f_d represents a path in which the light has been Doppler shifted, and u is the velocity of the moving reflector. When the light

reflected from the moving surface is recombined with light from the original laser, a beat frequency is generated. Our ability to resolve the moving reflector's velocity relates directly to how well we can resolve the beat frequency:

$$f_b \sim f_0 * \frac{2u}{c} \tag{1}$$

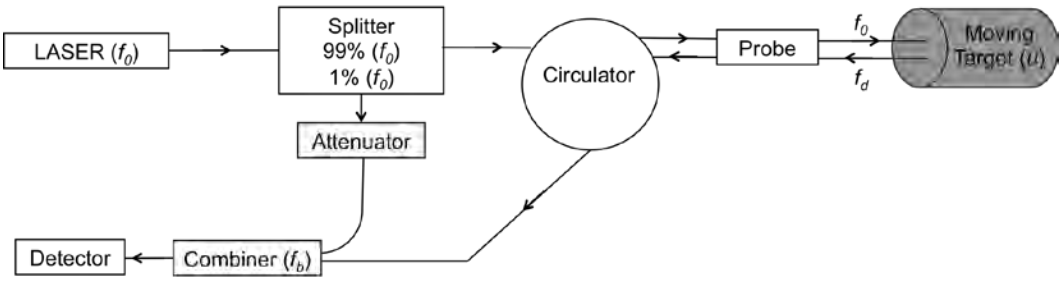

Fig. 1 A schematic of a PDV system.[1]

where f_b is the beat frequency and c is the speed of light. In the practical case where our dynamic range is limited by the bit-depth of the digitizer, best resolution occurs where the peak-to-valley magnitude of the beat frequency changes the greatest percentage of the full dynamic range. Figure 2 depicts example beat frequencies generated by combining 2 sinusoidal waves with frequency of the one reduced 2% from that of the original. In panel A, the sinusoidal waves had the same amplitude; in panel B the one sinusoidal wave had an amplitude equal to one-half the original; and in panel C the one sinusoidal wave had an amplitude equal to one-tenth the original. It becomes obvious that in the case where the amplitudes are nearest to equal (panel A), that the percent change of the dynamic range is the greatest (100% when exactly matched), and lessens as the amplitudes of the 2 waves differ. Therefore, when making PDV measurements, we desire to predict the amplitude of the reflected light so that we can select the amplitude of the unshifted light that we combine at the detector. This is accomplished in practice by adjusting an attenuator to control the intensity of unshifted light.

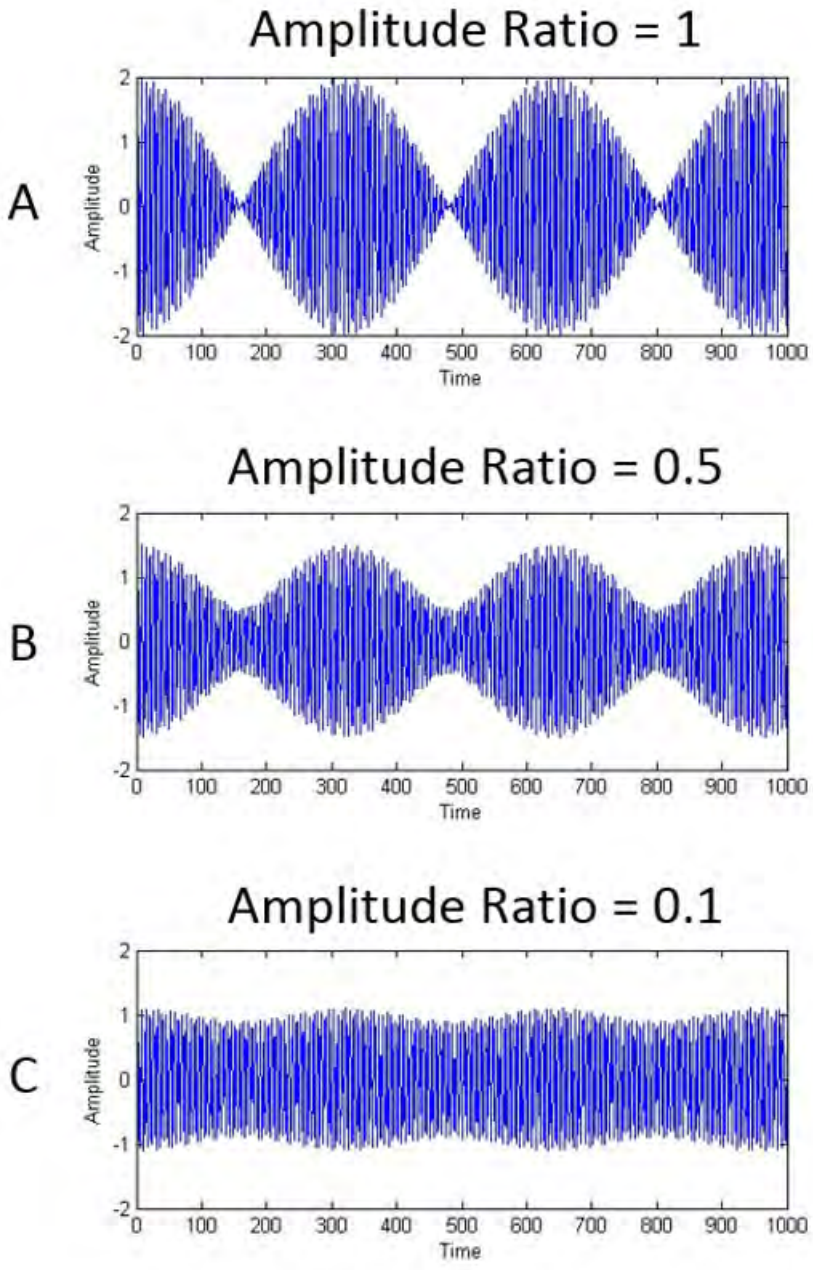

Fig. 2 Example of beat frequencies generated by adding 2 sinusoidal waves in which the frequency of the one wave was reduced by 2% from the original. In example A the sinusoidal waves had the same amplitude, in example B the one sinusoidal wave had an amplitude equal to 1/2 the original, and in example C the one sinusoidal wave had an amplitude equal to 1/10 the original.

The intention of the work described in this report is to provide quantified surface reflection measurements of 1.55-µm light from numerous materials and surface finishes to help predict the reflected intensity of Doppler shifted light one can expect in scenarios where the entire surface does not yield or undergo a phase or

chemistry change. The data are summarized over a range of angles from normal to 80°. Finally, the surface preparations are characterized using optical microscopy and surface profilometry, and generalizations are concluded about how surface texture relates to surface reflections for the different materials.

2. Experimental

To quantify potential PDV surface reflections, materials with multiple surface preparations were illuminated with laser light, and the reflected signature was measured as a function of angle with respect to the surface normal. To replicate the movement of a surface that occurs in PDV measurements, the samples were mounted to the end of a rod that was coupled to the cone of a speaker. The speaker was issued a 50-Hz frequency, which oscillated the surface over a distance on the order of 0.5 mm while the measurement was acquired. The mean value of the reflected power was reported.

During the acquisitions, the sample surfaces were illuminated with 0.0125 W of 1.55-μm light that was generated from an IPG ytterbium fiber laser (model ELR-2-1550-LP-SF). The light was projected to the surfaces through open air using a graded index of refraction lens pigtail (AC Photonics 1CL15A070LSD01) that was mounted approximately 60 mm from the material surfaces. The lens system generated a collimated beam with a 0.5-mm spot diameter. A Coherent Field Mate paired with an OP-2 IR Germanium optical sensor was placed approximately 50 mm behind, and 1.5° above the lens, which measured the total reflected power of the light with ±1-nanowatt resolution.

The entire system was mounted on a circular translating track so that measurements of materials prepared with multiple finishes could be assessed at any angle. The samples of varying thickness were oriented at the center of the circular track's 152.4-mm radius using a translation stage to ensure that the illuminated spot remained localized as the incident angle changed. For practicality, measurements of the incident and reflected light were acquired using 5° increments to form curves of reflected power versus angle for each finish. Figure 3 shows an optical photograph of the setup used to acquire the measurements at normal and 45° incidences.

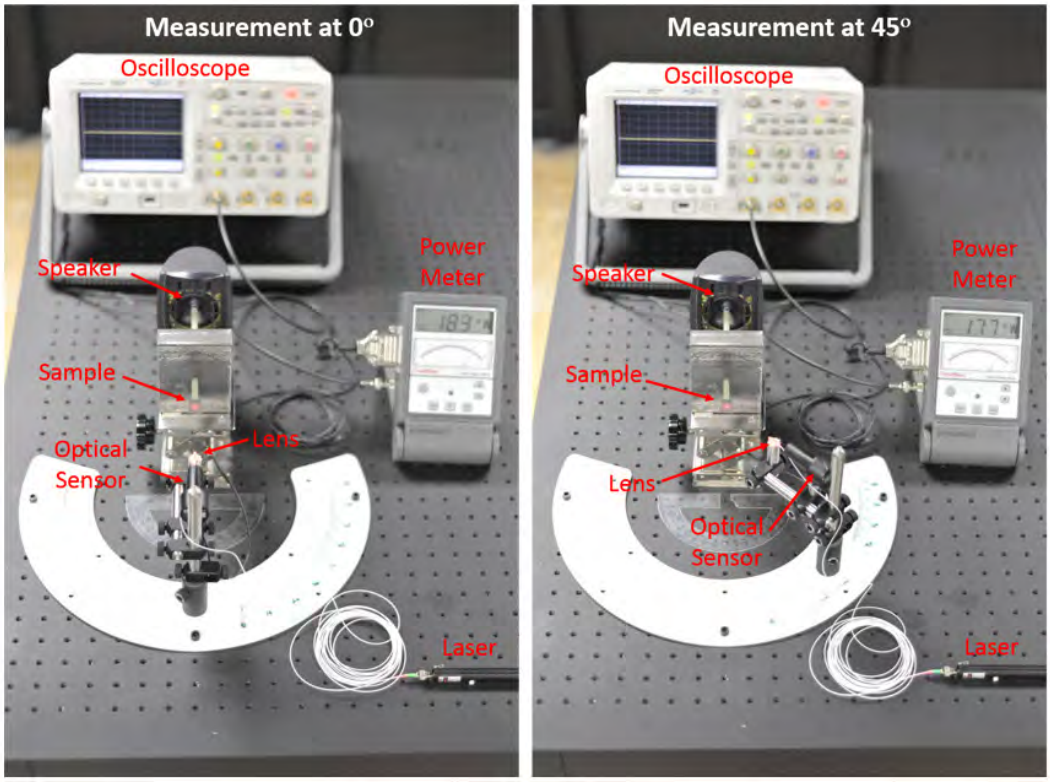

Fig. 3 Optical photograph of the setup used to acquire the measurements at normal and 45° incidences. In these photographs, a visible red laser was used so the illumination spot on the sample can be visualized. In the real experiments, an infrared laser was used.

Surface preparation depended on the material being tested. Generally, specimens were prepared with a particular surface finish in nominally 75- × 75-mm slabs for uniformity of the finish. The material was then cut to 10- × 10-mm squares for testing, which allowed ample room so that the measurements were not corrupted by edge effects. Characterization of the surface texture was documented using optical microscopy and surface profilometry. The optical microscopy was acquired using an AmScope 10–40× stereo microscope fitted with a 5-megapixel charge coupled device (CCD) camera and IS Capture software. The surface profilometry was accomplished using a Phase II+ SRG-4500 surface roughness tester paired with a diamond stylus. This tester was capable of measuring surface deviations of 0.01 ± 40 μm with 10% accuracy and 6% repeatability. Reported surface parameters include the roughness average, Ra, the root mean square roughness, Rq, the average maximum height of the profile, Rz, and the spacing of profile irregularities, Rs, as defined by the American Society of Mechanical Engineers Standard.[7]

3. Surface Finishes

As-is: This finish may include significant surface oxidation as most of the materials were acquired from legacy stocks that were stored in nonenvironmentally controlled warehouses. Materials were cut using a horizontal saw that flowed Cimcool Cimtech 495 undyed metalworking fluid. The fluid was removed using compressed air and evaporation.

Machined (Fly Cutter): As-is material was prepared with a machined finish using a hand ground, 60°-triangular shaped, tool-steel bit. The bit, which was mounted using a 55-mm radius, was spun at 800 revolutions-per-minute (rpm) while the as-is material was fed under it at a rate of 1.27 mm/s (3 inches/min).

Painted: As-is materials were coated with 2 coats of automotive gray enamel primer (flat). The paint was spray applied on from a 12-oz aerosol can using 2 coats with 15-min intercoat cure time.

Sandblasted: As-is materials were blasted with 80-grit garnet propelled by 80-psi compressed air using random motions until visual inspection identified complete removal of oxidized surfaces.

Sanded: As-is or surface ground materials were hand sanded using a "figure-8" pattern with 240 3M Wetordry Tri-M-ite A weight paper. To apply the finish, the samples were held in a pup-fixture while the "figure-8" motion was repeated 40 times.

Saw cut: As-is material cut using a band saw with appropriate toothed blade.

Ground surface: As-is material ground using a Chevalier FSG-3A818 surface grinding machine. The finished surface was prepared using an approximately 125-mm-diameter silicon carbide grinding wheel spinning at 2,850 rpm while the material was fed under it at 500 mm/min and 3-mm lateral steps.

Waterjet cut: As-is material cut using a Flow International two axis water jet. The water jet used Barton Abrasive 80 HPA garnet and a 50 horsepower intensifier pump, which pressurized the water to 65,000 psi for cutting.

4. Results and Discussion

The Table summarizes the materials and surface finishes from which reflected power measurements were made. Figures 4–7 show compilations of reflected power off of metals as a function of surface finish. The individual power reflectance for all materials, along with surface microscopy and surface profilometry parameters can be found in the appendixes assigned within the

Table. In all cases, the law of reflection coupled with a coefficient of reflection is sufficient to explain the results obtained. When a surface is finished with a smooth, flat finish the reflection pattern tends toward that of a specular reflector. When the finish is textured, the reflection pattern tends toward a diffuse reflection (Fig. 8).

Table Summary of materials and finishes measured

Material	As-is	Fly-cut	Painted	Sand Blasted	Sanded (240 Grit)	Saw Cut	Surface Ground	Water-Jet Cut	Appendix
RHA	x	…	x	x	x	…	x	…	A
Al 6061	x	x	x	x	x	…	x	…	B
Ti 6Al-4V	x	…	x	x	x	…	x	…	C
Mg	x	x	…	x	x	…	x	…	D
Helmet Inside	x	…	…	…	…	…	…	…	E
Helmet Outside	x	…	x	…	…	…	…	…	E
SS II	x	…	…	…	…	x	…	x	F
HB-26	x	…	…	…	…	x	…	x	G
Al_2O_3	x	…	…	…	…	…	…	…	H
Polyethylene	x	…	…	…	…	x	…	…	I
Kevlar	x	…	…	…	…	…	…	x	J
Mild Steel	…	…	…	…	…	x	…	…	K

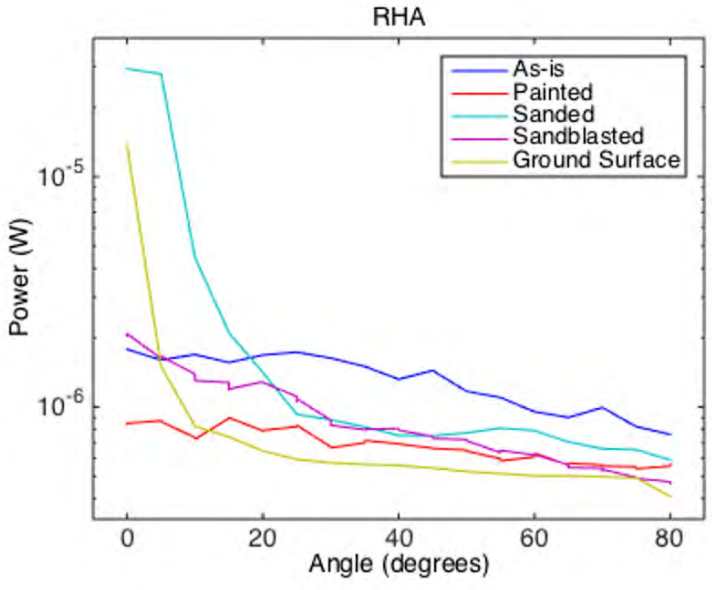

Fig. 4 Reflected power measurements as a function of incident/detection angle for RHA prepared with multiple surface-finishes

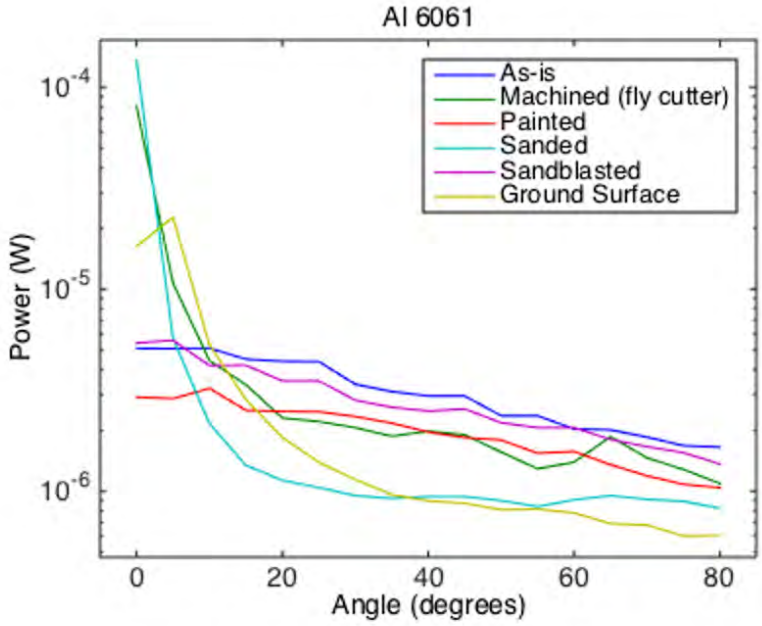

Fig. 5 Reflected power measurements as a function of incident/detection angle for Al 6061 prepared with multiple surface-finishes

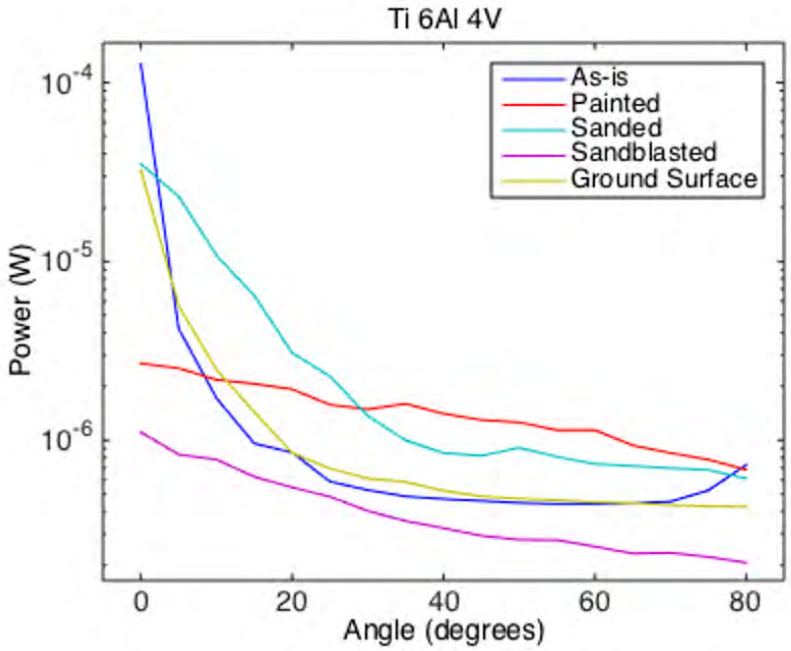

Fig. 6 Reflected power measurements as a function of incident/detection angle for Ti 6AL 4V prepared with multiple surface-finishes

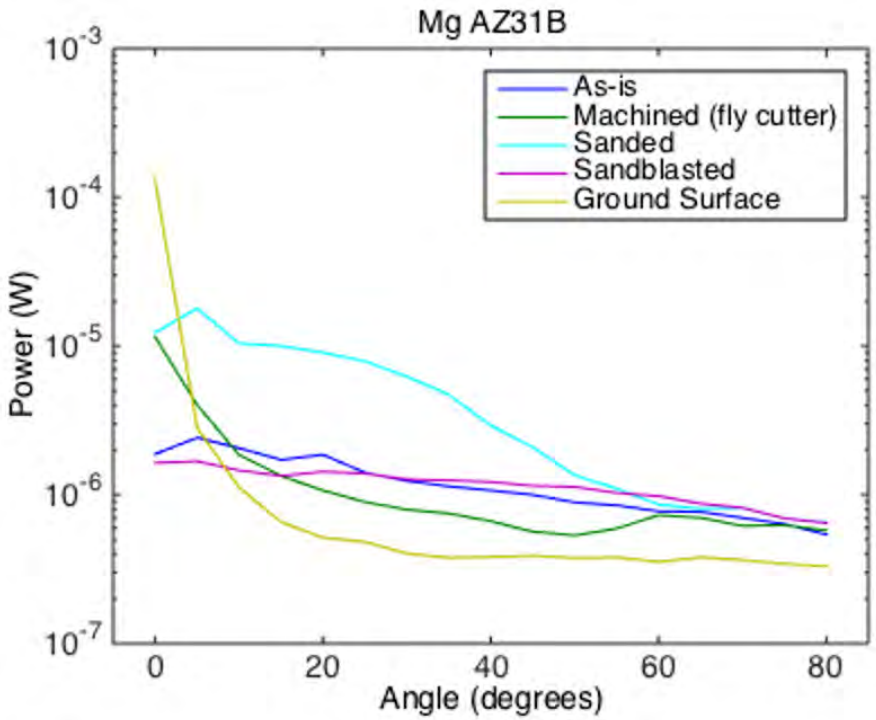

Fig. 7 Reflected power measurements as a function of incident/detection angle for Mg AZ31B prepared with multiple surface-finishes

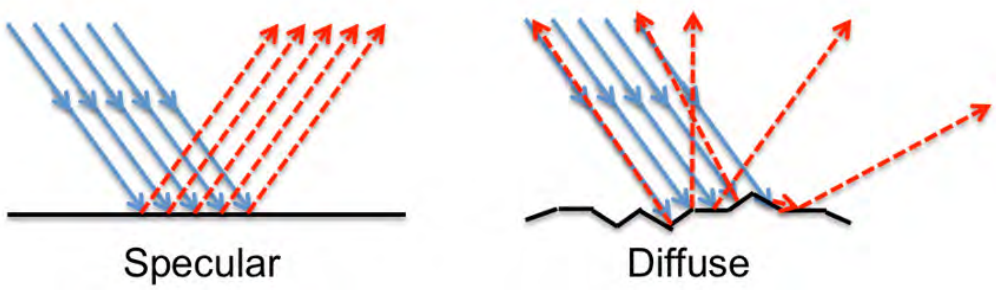

Fig. 8 Illustration depicting differences between a specular reflector (left) and a diffuse reflector (right). Solid blue arrows portray incident light rays and dashed red arrows portray reflected light rays.

In our tests, the metals prepared with relatively smooth, flat surface finishes (ground surface, machined, and sanded) reflected most of the light in a pattern that peaked when the light was incident and detected normally and reduced significantly as the angle of incidence and detection became more obtuse. This is in accordance with aforementioned hypothesis because the transmitter and detector are oriented at approximately the same location. At the off-normal incidences, a significant portion of the light is reflected to a position on the opposite side of the surface normal (specular), and only a small portion of light

from a diffuse component makes it back to the detector. These surface preparations would be preferred when attempting to make PDV measurements where normal incidences are accessible, because the total intensity of the Doppler shifted signal would be maximized. When the surfaces were prepared with more texture (sandblasted, painted, or typically as-is), the reflection was more diffuse in nature. This produced a greater retention of reflected power at obtuse angles, and therefore would be a preferred surface finish when trying to maximize reflected signal for measurements such as PDV, when non-normal incidences are required.

Here we note one peculiarity—if the surface finish is prepared using a method that creates surface area at a preferred angle, the intensity of light reflected and detected will increase when the transmitter/detector pair is oriented at the complement of the angle in our test setup. This can be observed when the surface is prepared with a method such as machined with a fly cutter, which makes multiple triangular grooves on the surface. In both the Al 6061 and Mg surfaces prepared this way, the measured reflected power increased at an angle of 60–65°. Surface profilometry confirmed that the triangular grooves inscribed by this machining method had a 30° angle with respect to the surface normal.

Figure 9 depicts a compilation of the reflected power measurements as a function of angle made on multiple metals prepared with sandblasted finishes. Because the sandblasted finishes produce similar surface textures on all materials (diffuse with random surface angles), and removes most surface impurities, comparison of the reflected signatures allows for an estimation of the relative reflection coefficient. This technique for estimating the reflection coefficient is in good agreement with the computed normal reflection, R, of elemental Al (97.8%), Fe (72.5%, the main constituent of RHA), and Ti (59.6%):[8]

$$R = \frac{(n_1{}^2 - n_2{}^2) + k_2{}^2}{(n_1{}^2 + n_2{}^2) + k_2{}^2} \tag{2}$$

where the n's are the indices of refraction of the materials through which the electromagnetic wave propagates and k is the extinction coefficient of the reflecting medium. This technique provides a useful tool for estimating reflection coefficients for unique alloys and materials to which the indices of refraction and extinction coefficients are unknown.

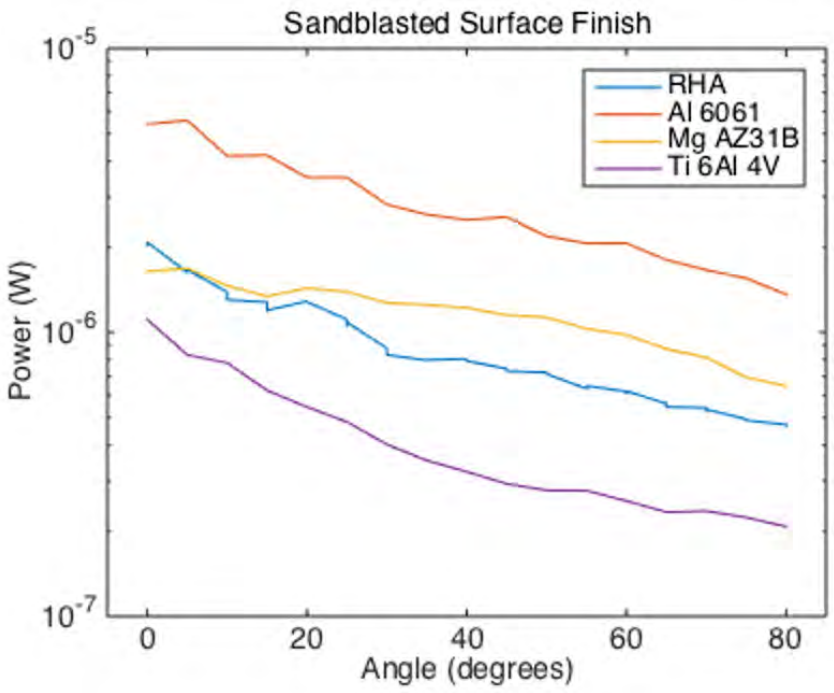

Fig. 9 Reflected power measurements as a function of incident/detection angle for multiple surfaces prepared with sandblasted finishes. The trend in reflected power agrees well with the normal reflectance computed for elemental Al (97.8%), Fe (72.5%, the main constituent of RHA), and Ti (59.6%).[8]

5. Conclusions

This work described in this report measured the intensity of 1.55-μm light reflected from numerous materials prepared with varying surface finishes. The data can be used as a guide for conducting Photon Doppler Velocimetry measurements, which necessitates a prediction of the quantity of Doppler shifted light that will be reflected from a surface to optimize the measurement. It was observed in all cases that the power of reflected light could be sufficiently explained by applying the law of reflection coupled with a coefficient for the material's reflection. Identifying the surface texture of the reflecting specimens can therefore approximate a prediction of the intensity of light reflected as a function of incident/detection-angle. Most importantly, this work includes appendixes of many common materials of varying surface preparations, a surface characterization, and the reflected power measurements as a function of angle. These conclusions and the applicability of the measurements are only valid for surfaces where accelerations are insufficient to cause the surface to yield or chemically change across its majority.

6. References

1. Strand OT, Goosman DR, Martinez C, Whitworth TL, Kuhlow WW. Compact system for high-speed velocimetry using heterodyne techniques. Rev. Sci. Instr. 2006;77:083108.

2. Ao T, Dolan DH. SIRHEN: a data reduction program for photonic Doppler velocimetry measurements. Albuquerque (NM) and Livermore (CA): Sandia National Laboratories; 2010 Jun. Sandia Report No.: SAND2010-3628.

3. Doppler CJ. Über das farbige Licht der Doppelsterne und einiger anderer Gestirne des Himmels. Abhandlungen der Koniglich Bohmischen Gesselschaft der Wissenschaften, 1842;1:465–482.

4. Randow CL, Zellner, MB, Analysis of an underbody blast from a computational and experimental perspective. Report No.: ARL-TR-XXXX (will be submitted in Aug 2015).

5. Schuster BE, Aydelotte BB, Leavy RB, Satapathy S, Zellner MB. Concurrent velocimetry and flash x-ray characterization of impact and penetration in an armor grade ceramic. HVIS accepted.

6. Zellner MB, Vunni GB. Conference Proceeding of Hypervelocity Impact Symposium; Baltimore (MD): 2012 Aug 17–21. Report No.: ARL-TR-5961. Procedia Engineering. 2013;58:88–97.

7. Surface Texture (Surface Roughness, Waviness, and Lay). ASME. B46.1-2002.

8. Weaver JH, Frederikse HPR. Optical properties of selected elements. Within CRC handbook of chemistry and physics. 96th ed. 2015-2016. p. 12–126.

Appendix A. RHA Reflected Power Measurements as a Function of Angle, Surface Profilometery, and Optical Photography at 10-, 20-, and 40-Times Magnifications

This appendix appears in its original form, without editorial change.

Surface profilometry of RHA was acquired at two spots because of the significant texture variation across the surface, one that was deemed relatively rough as assessed by eye and one that was deemed relatively smooth as assessed by eye.

Finish: As-is

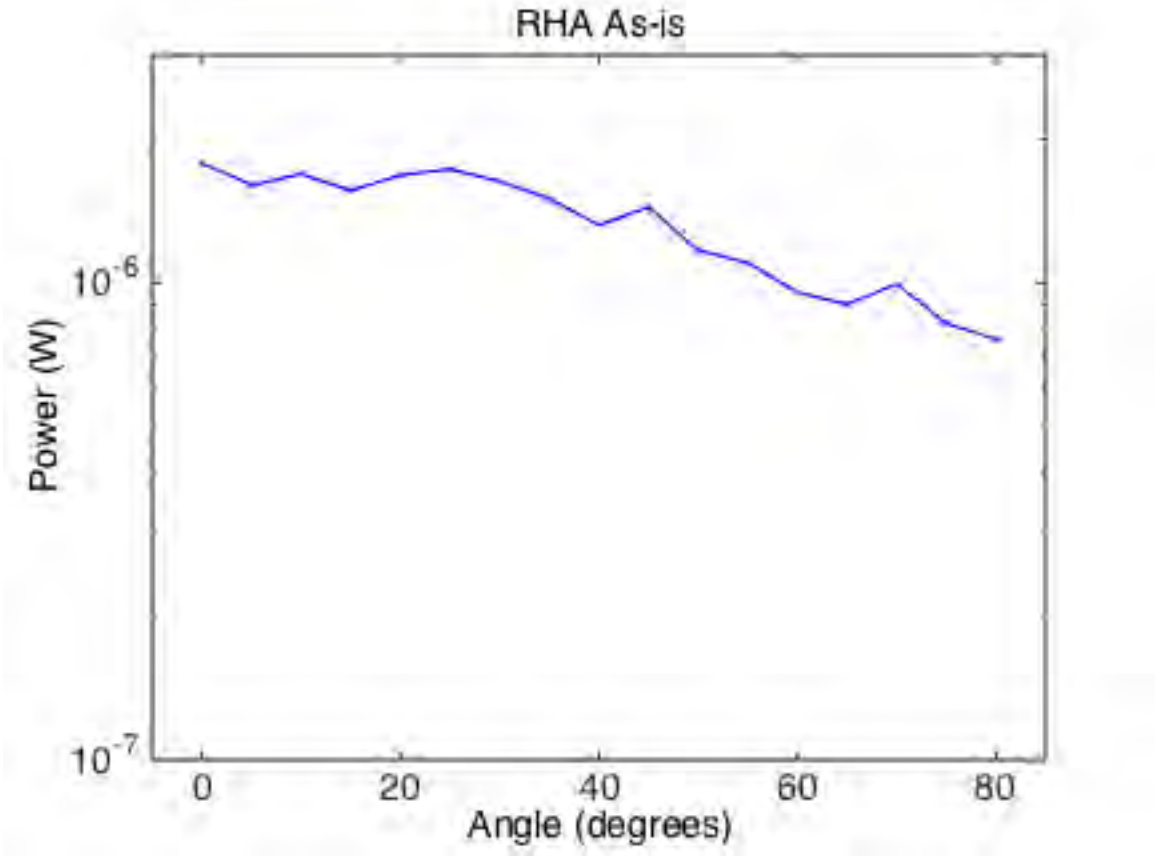

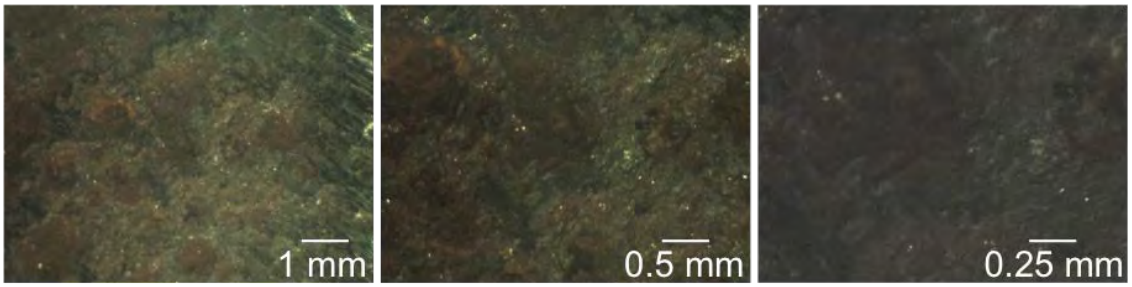

Ra (µm)	Rq (µm)	Rz (µm)	Rs (mm)
7.352	8.928	26.96	0.0370
4.840	5.971	16.46	.0331

Finish: Painted

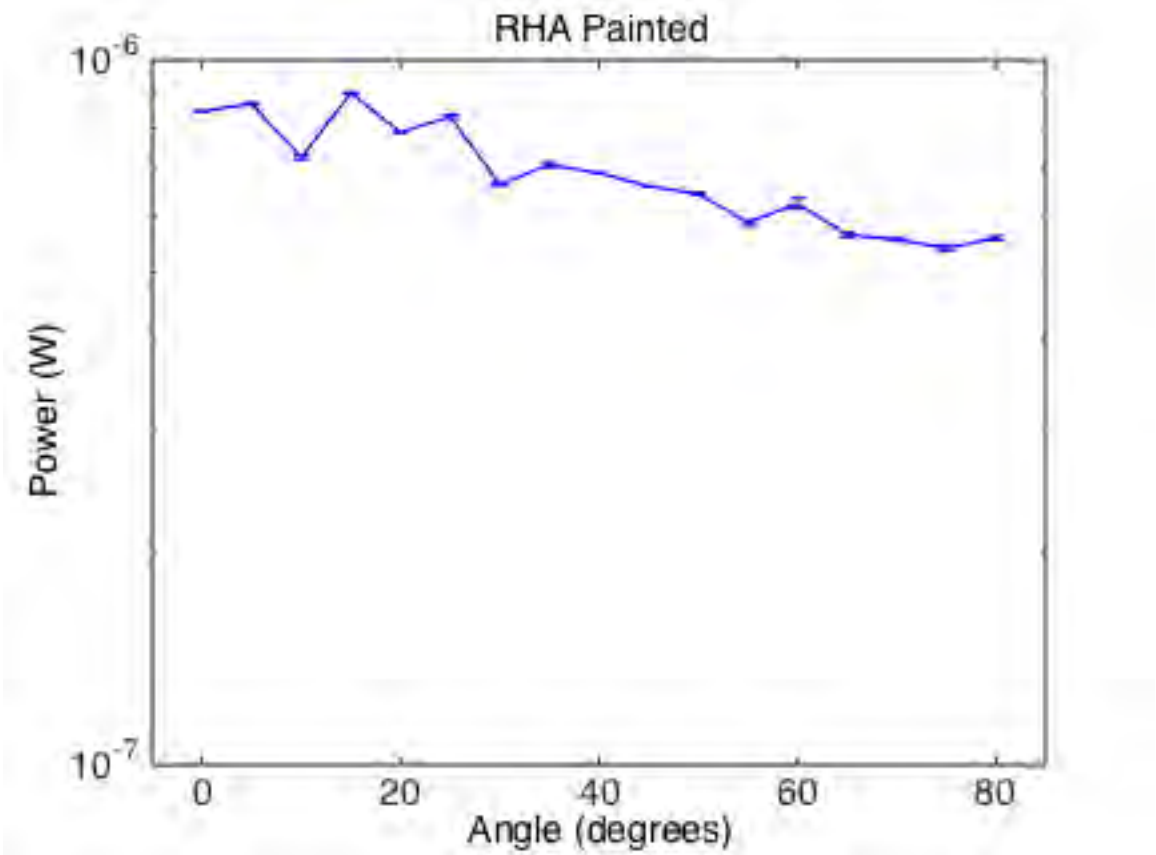

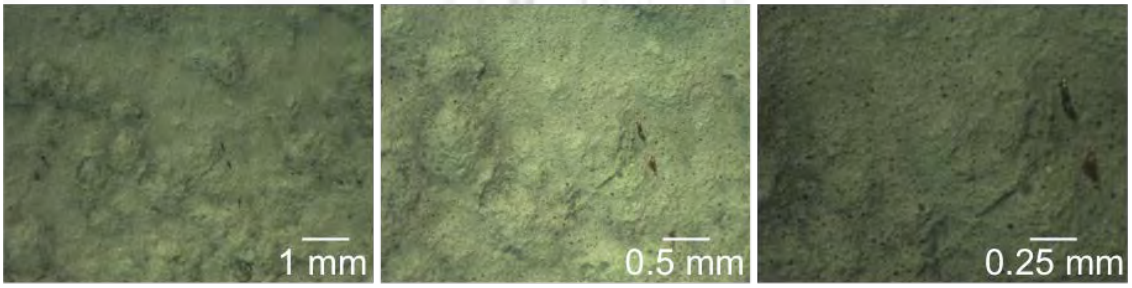

Ra (µm)	Rq (µm)	Rz (µm)	Rs (mm)
6.836	8.328	16.96	.044
3.514	4.38	8.171	.0250

Finish: Sandblasted

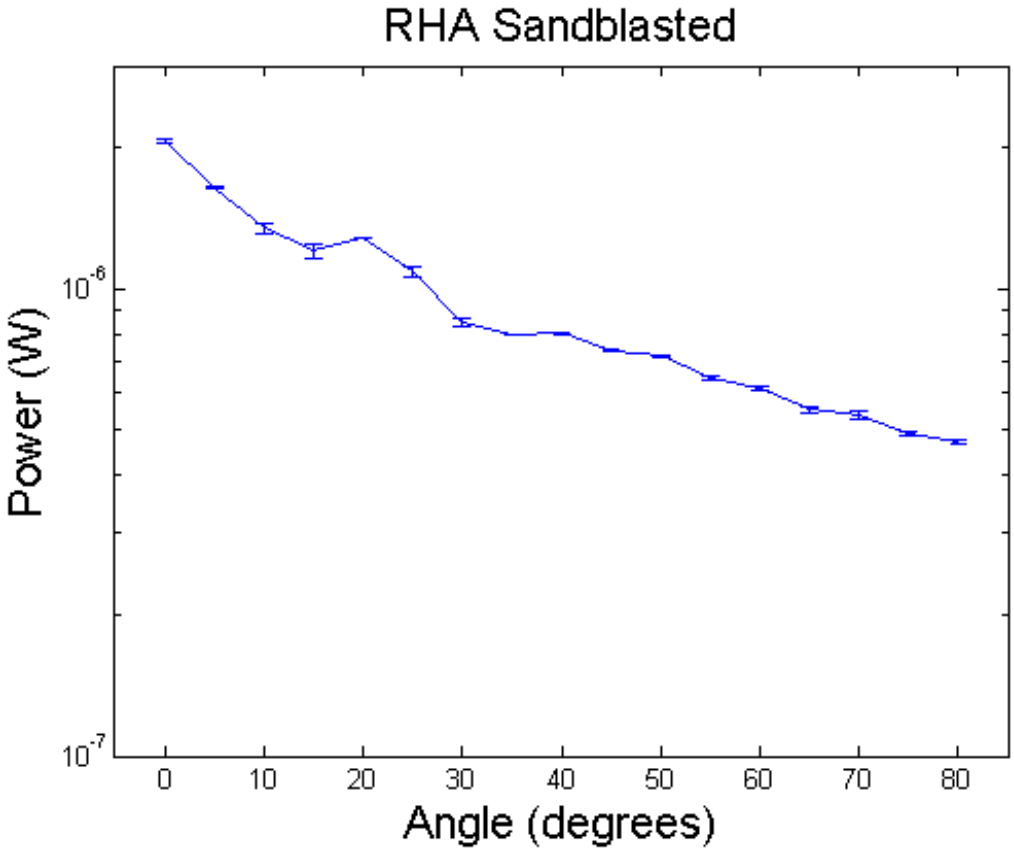

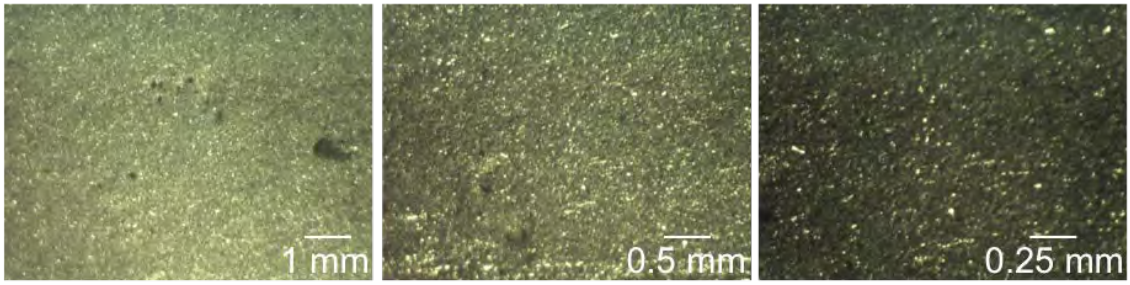

Ra (µm)	Rq (µm)	Rz (µm)	Rs (mm)
6.215	8.035	27.96	0.0279
2.365	2.925	11.53	.0309

Finish: Sanded

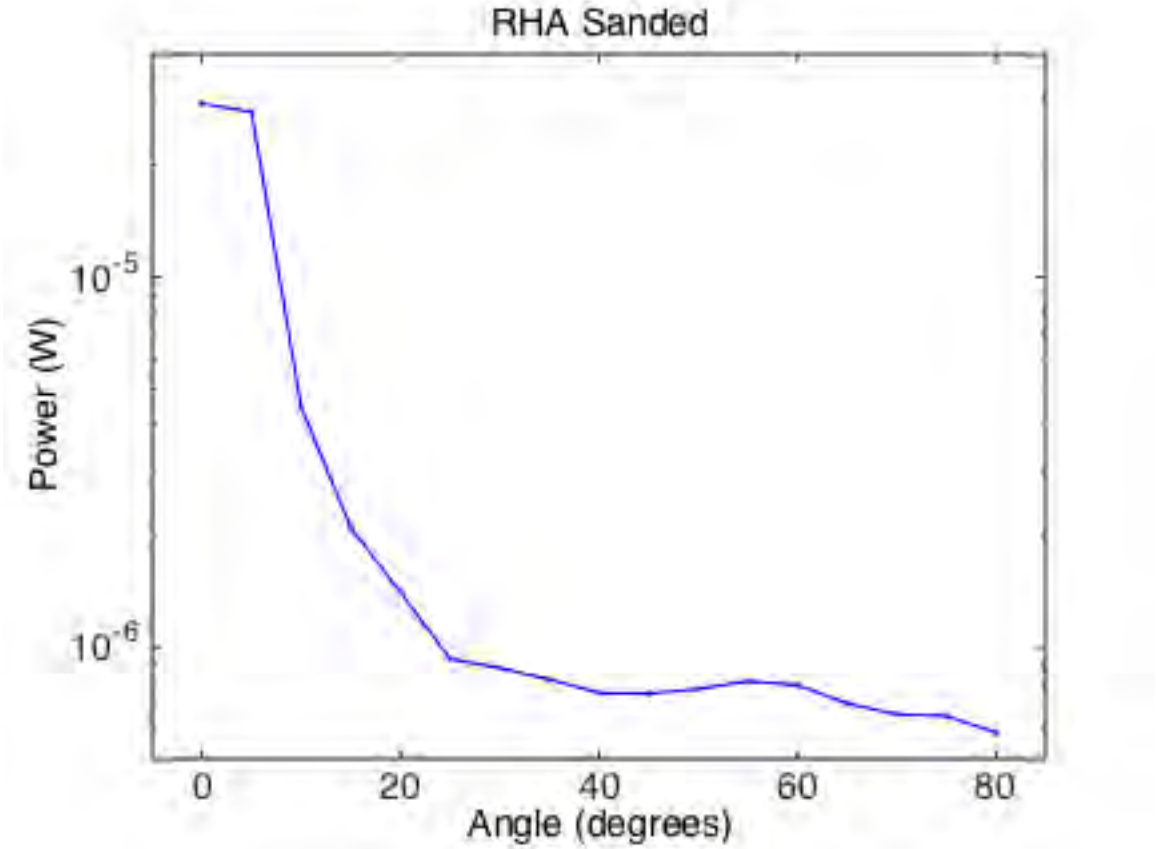

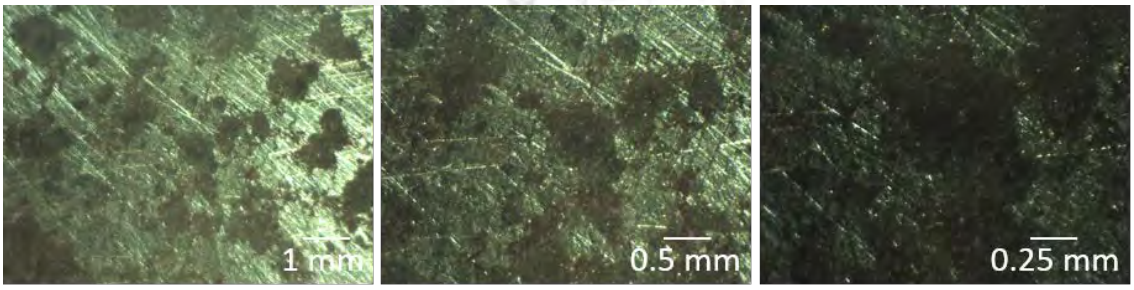

Ra (µm)	Rq (µm)	Rz (µm)	Rs (mm)
2.561	3.023	8.25	.0213
.581	.759	3.226	.0177

Finish: Ground Surface

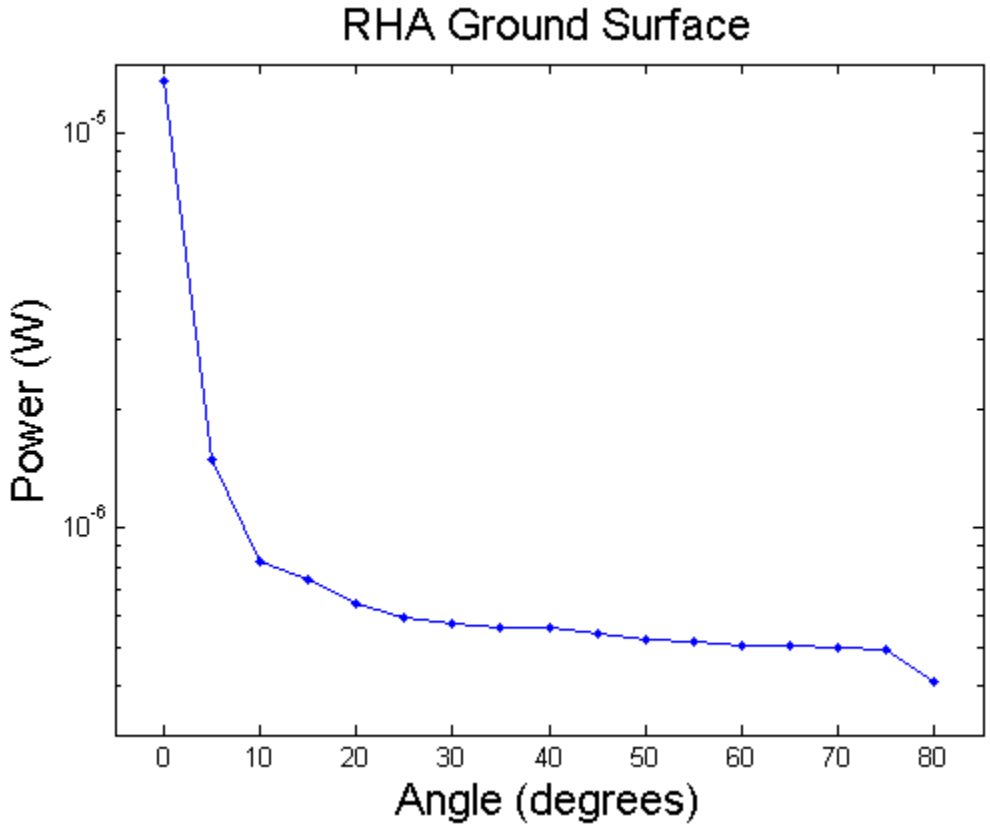

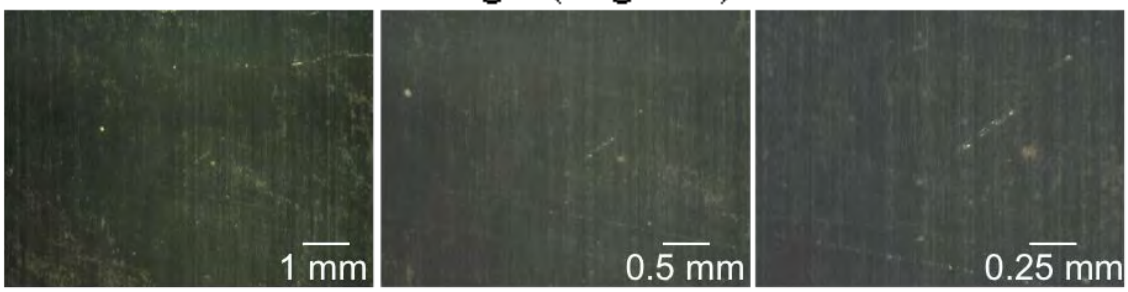

Ra (µm)	Rq (µm)	Rz (µm)	Rs (mm)
1.090	1.570	8.609	.0129
.512	.651	2.828	.0063

Appendix B. Al 6061-T6 Reflected Power Measurements as a Function of Angle, Surface Profilometery, and Optical Photography at 10-, 20-, and 40-Times Magnifications

This appendix appears in its original form, without editorial change.

Surface profilometry of Al 6061 was acquired at two spots because of the significant texture variation across the surface, one that was deemed relatively rough as assessed by eye and one that was deemed relatively smooth as assessed by eye.

Finish: As-is

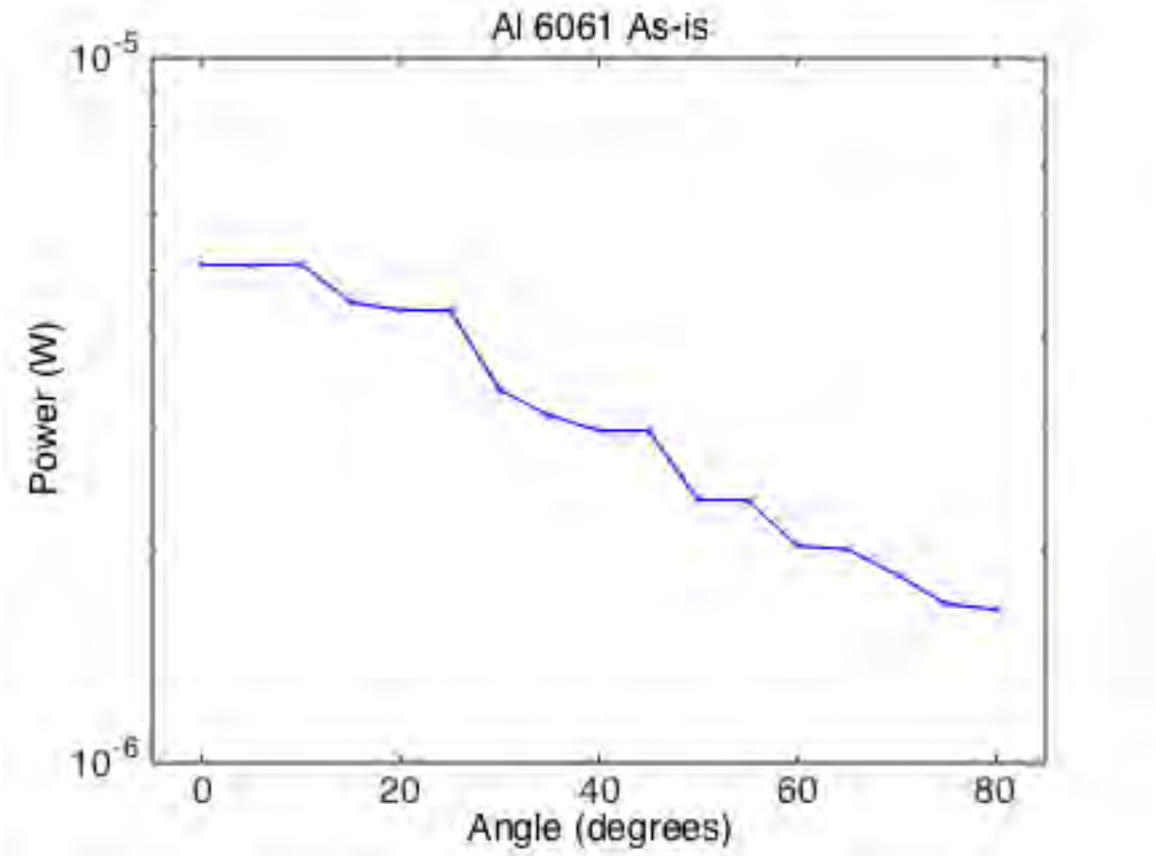

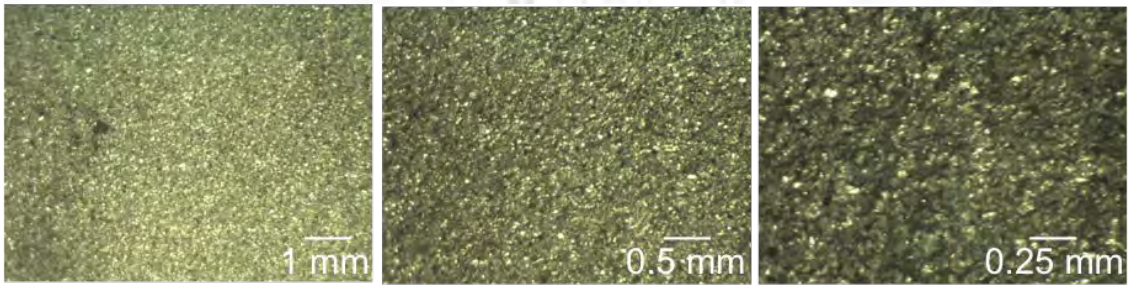

Ra (µm)	Rq (µm)	Rz (µm)	Rs (mm)
4.049	5.134	20.42	.0563
3.188	4.057	16.40	.0385

Finish: Machined (Fly Cutter)

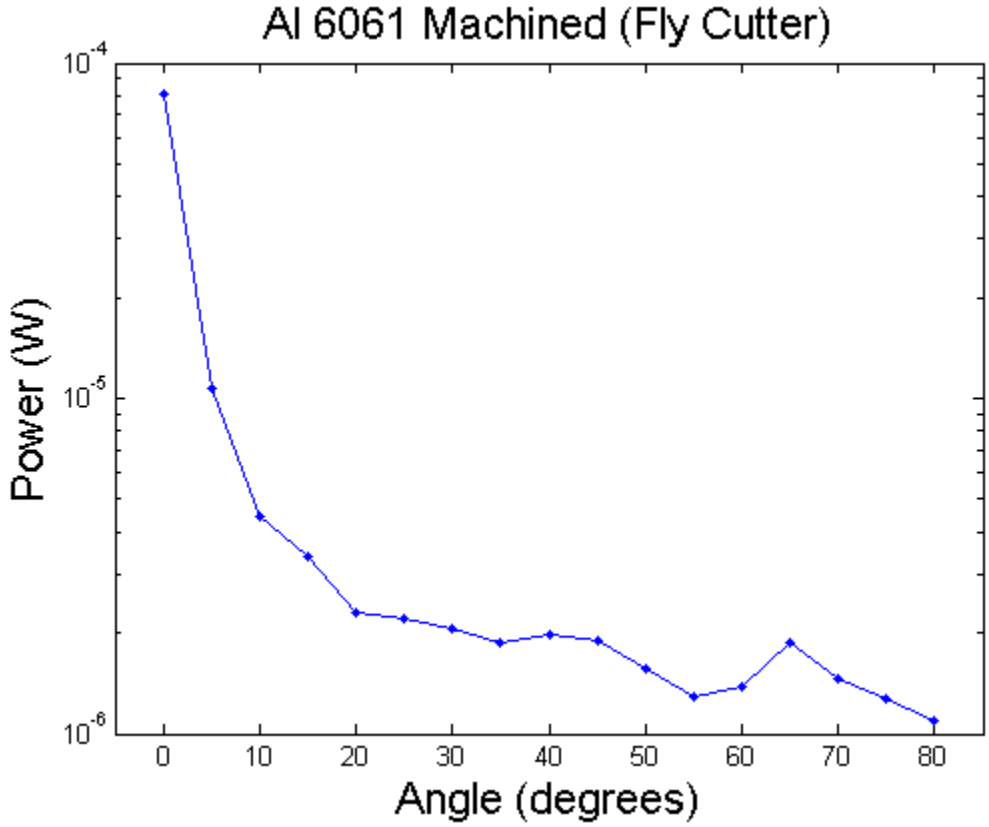

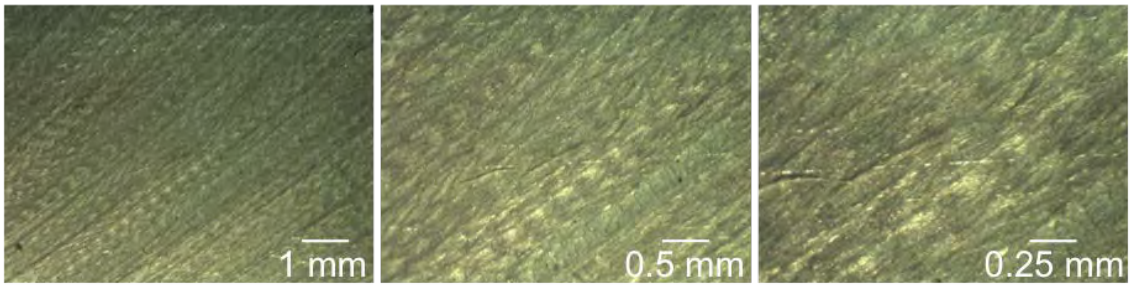

Ra (µm)	Rq (µm)	Rz (µm)	Rs (mm)
1.993	2.459	9.175	.0502
1.618	1.913	5.929	.0351

Finish: Painted

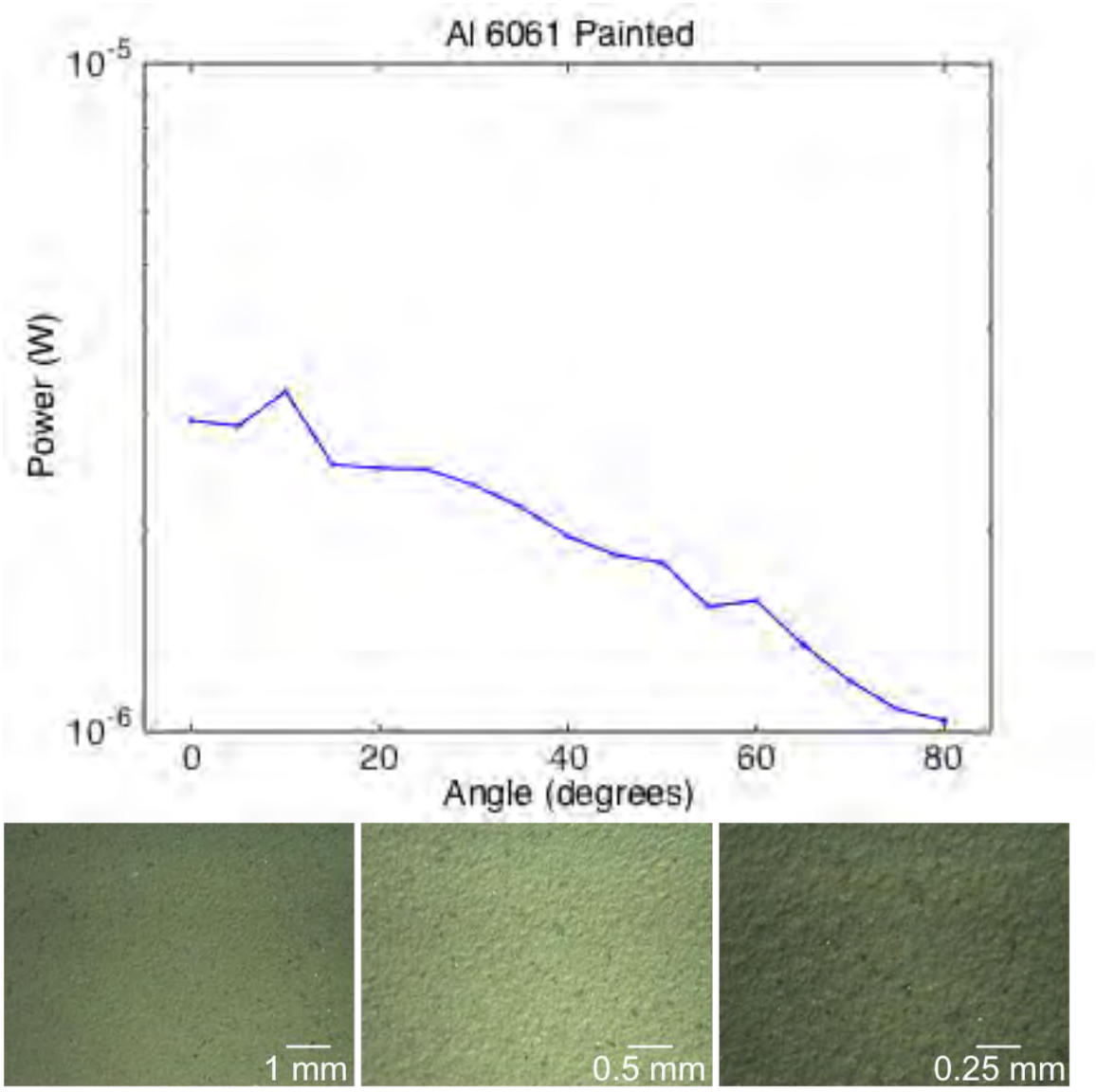

Ra (µm)	Rq (µm)	Rz (µm)	Rs (mm)
2.362	3.122	15.38	.0812
2.255	2.891	10.60	.0686

Finish: Sandblasted

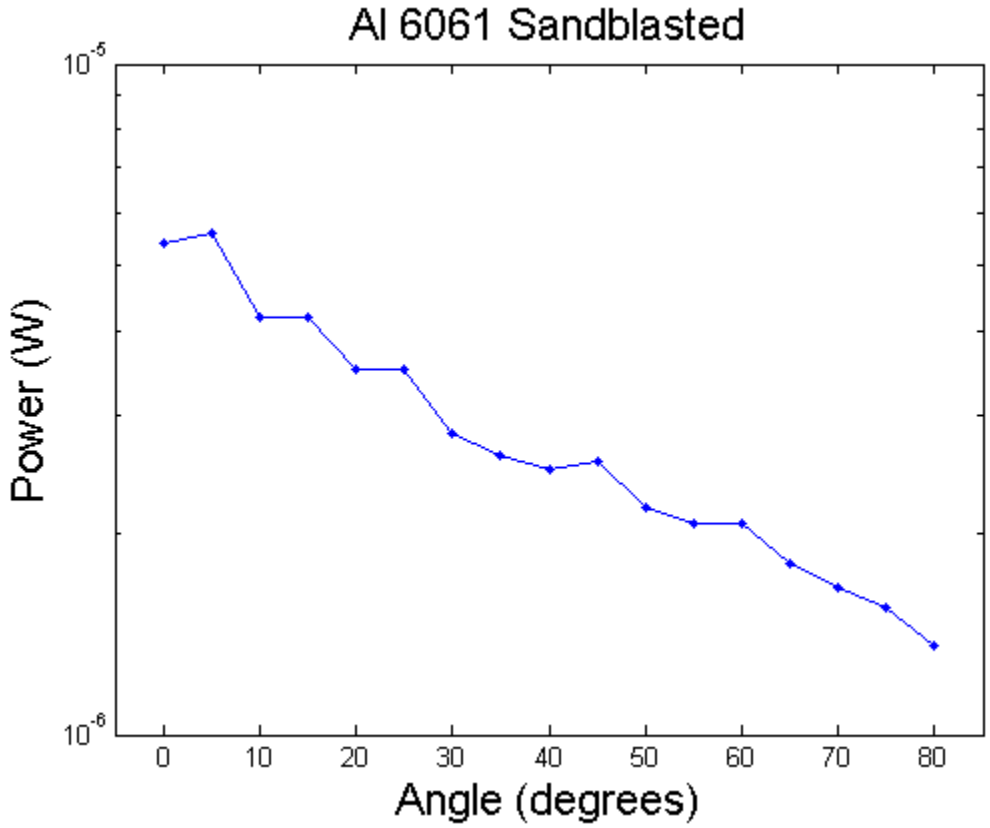

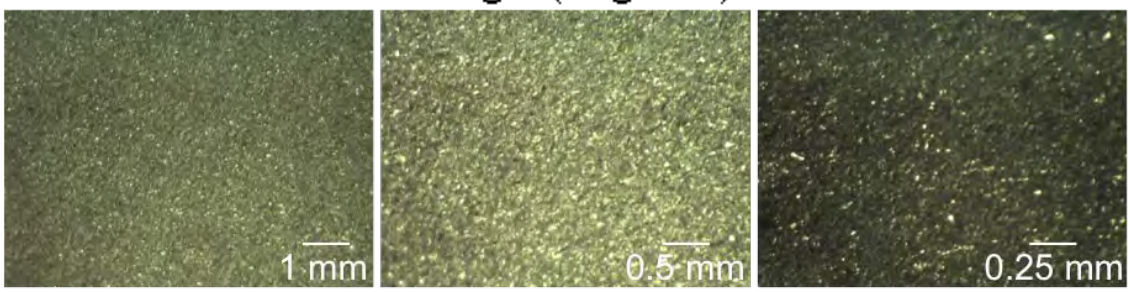

Ra (µm)	Rq (µm)	Rz (µm)	Rs (mm)
3.488	4.290	19.66	.0535
4.108	4.915	14.71	.0453

Finish: Sanded

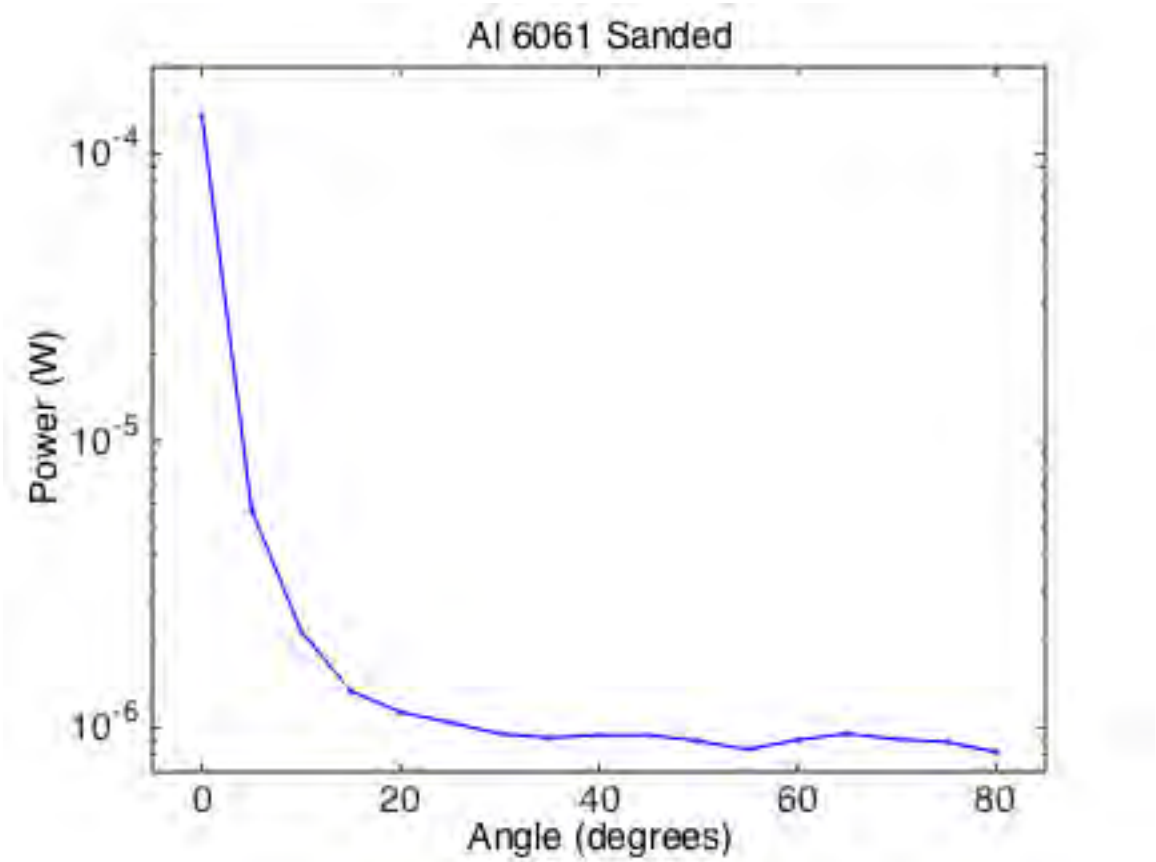

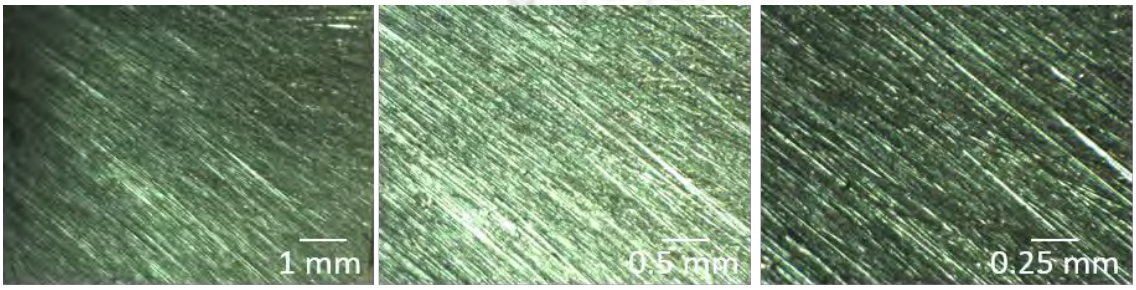

Ra (µm)	Rq (µm)	Rz (µm)	Rs (mm)
1.646	2.114	9.937	.0167
.829	1.065	4.718	.0204

Finish: Ground Surface

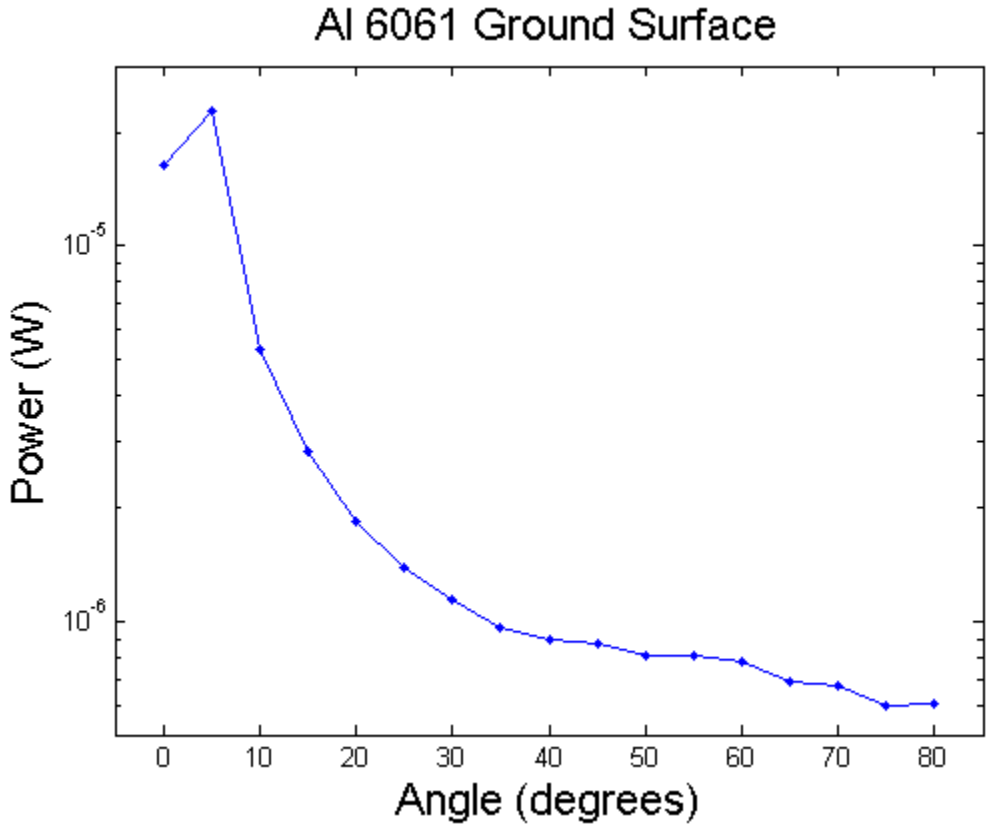

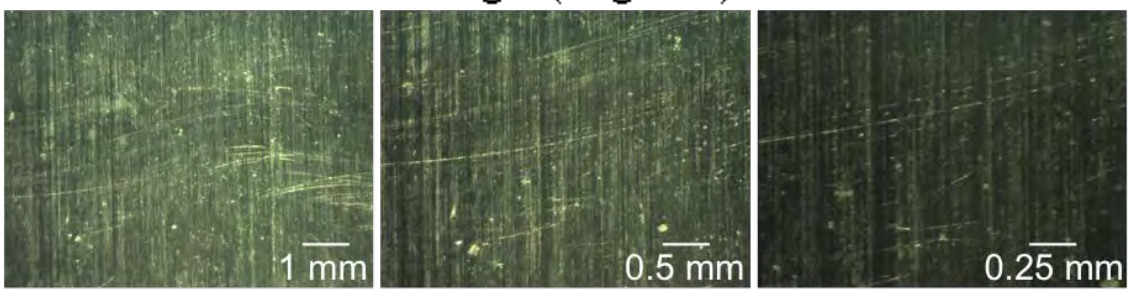

Ra (µm)	Rq (µm)	Rz (µm)	Rs (mm)
0.771	0.997	4.433	.0226
0.756	0.966	4.734	.0131

INTENTIONALLY LEFT BLANK.

Appendix C. Ti 6Al 4V Reflected Power Measurements as a Function of Angle, Surface Profilometery, and Optical Photography at 10-, 20-, and 40-Times Magnifications

This appendix appears in its original form, without editorial change.

Surface profilometry of Ti 6Al 4V was acquired at two spots because of the significant texture variation across the surface, one that was deemed relatively rough as assessed by eye and one that was deemed relatively smooth as assessed by eye.

Finish: As-is

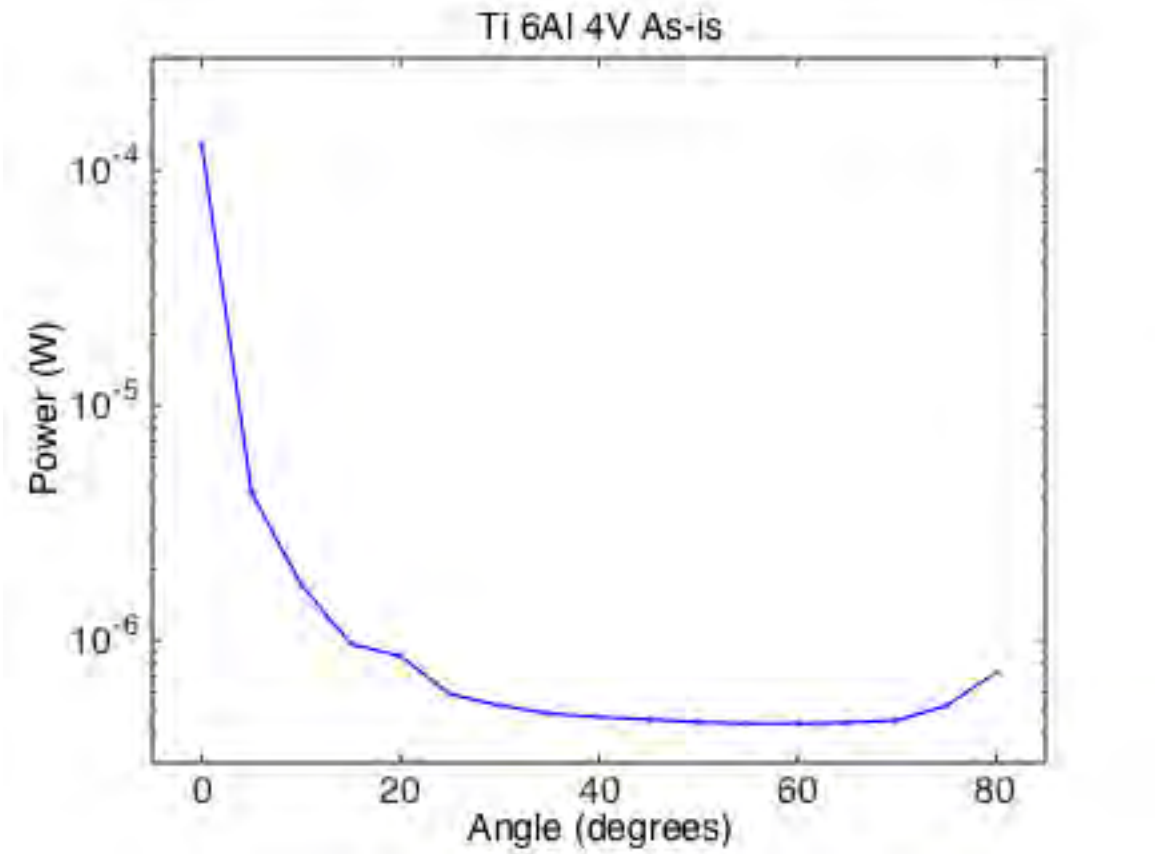

Ra (µm)	Rq (µm)	Rz (µm)	Rs (mm)
6.142	7.481	24.76	.0547
3.962	4.711	9.515	.0336

Finish: Painted

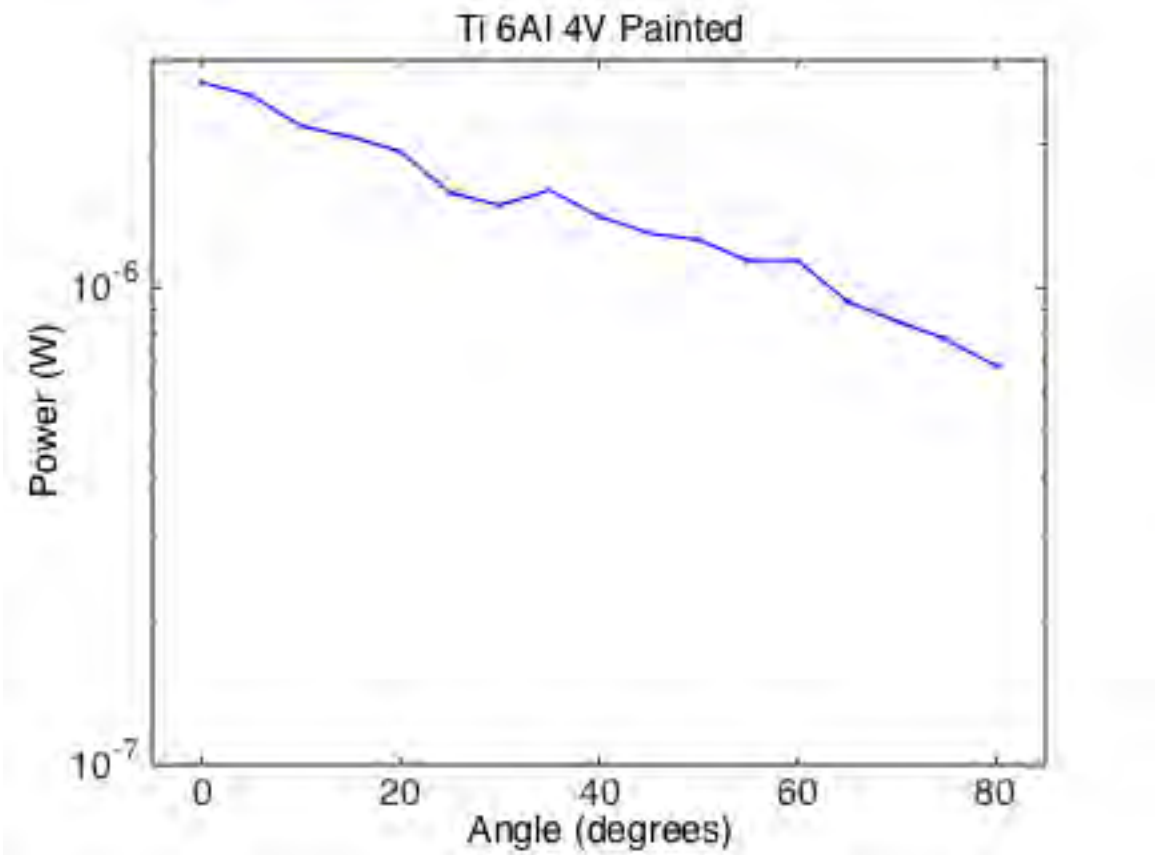

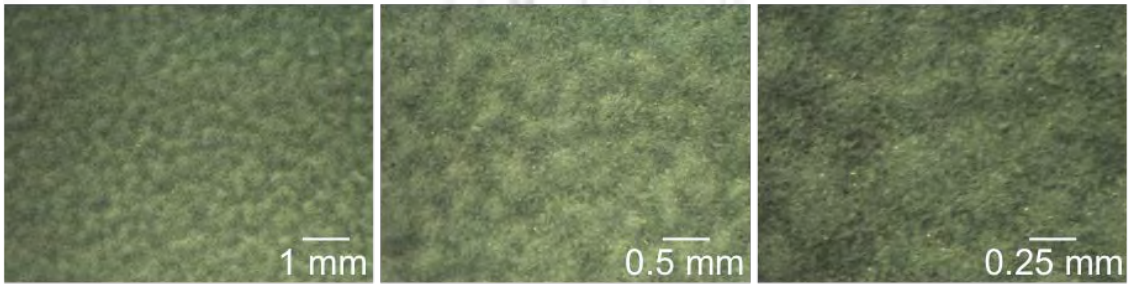

Ra (µm)	Rq (µm)	Rz (µm)	Rs (mm)
2.710	3.611	18.55	.0839
3.076	3.992	13.39	.0594

Finish: Sandblasted

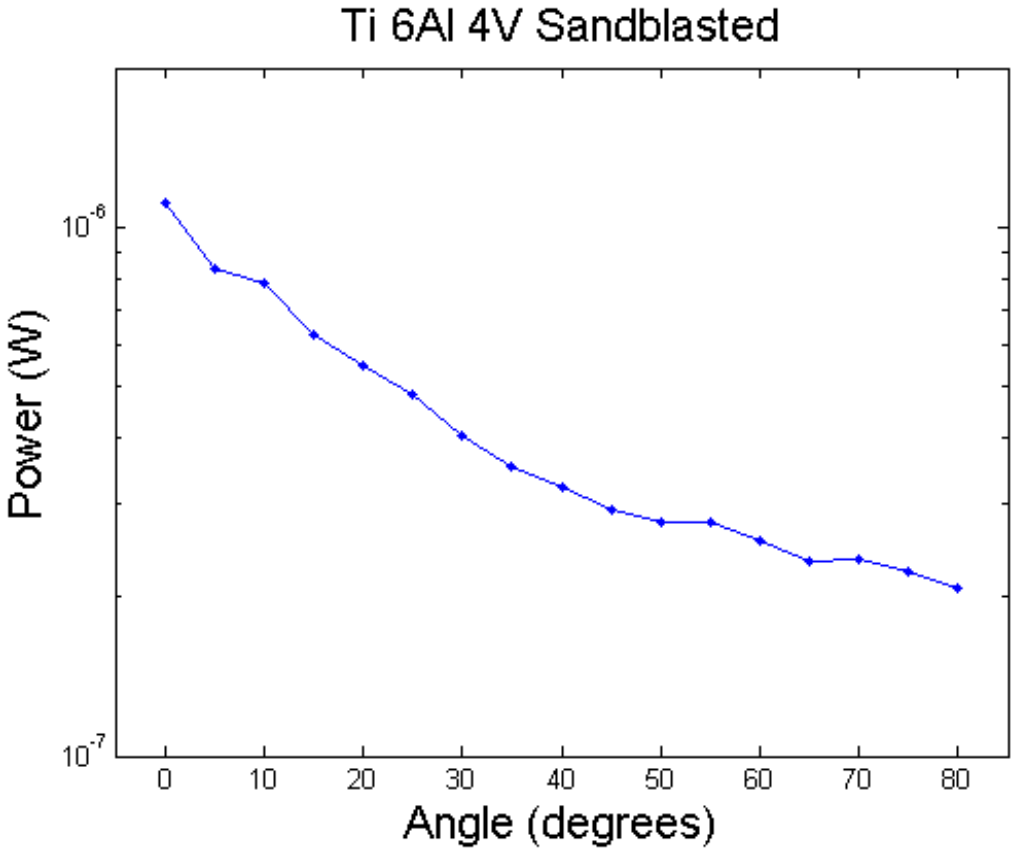

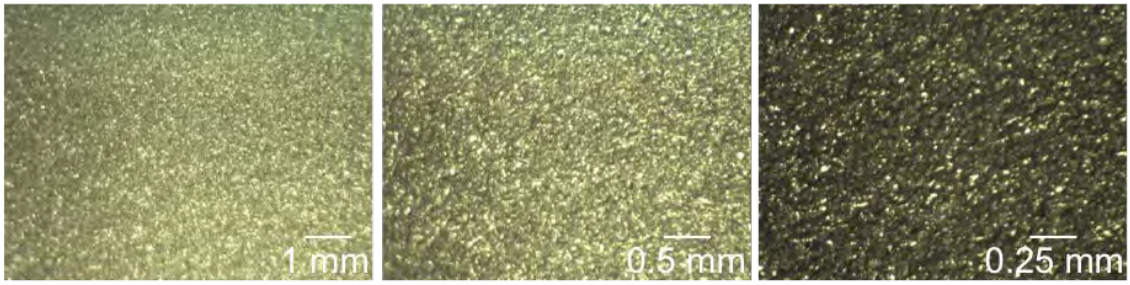

Ra (µm)	Rq (µm)	Rz (µm)	Rs (mm)
2.843	3.776	21.21	.0493
3.023	3.634	14.42	.0328

Finish: Sanded

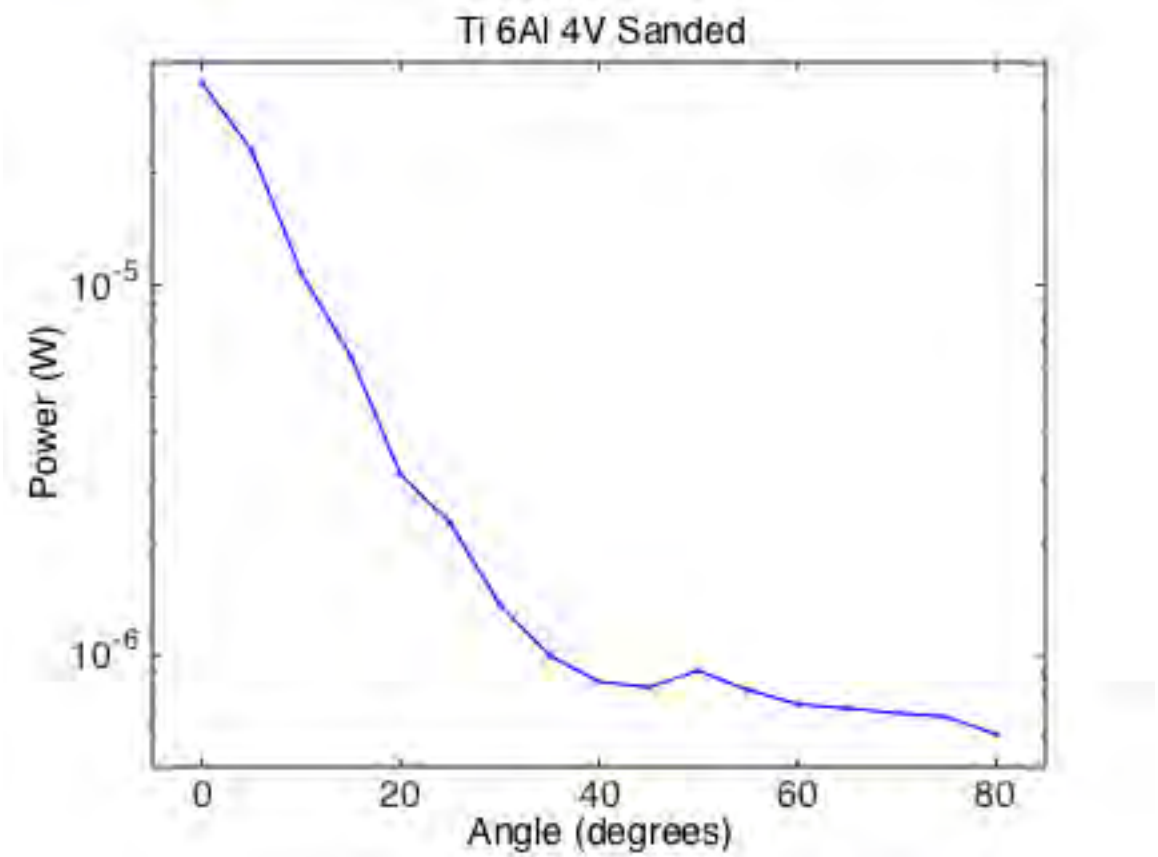

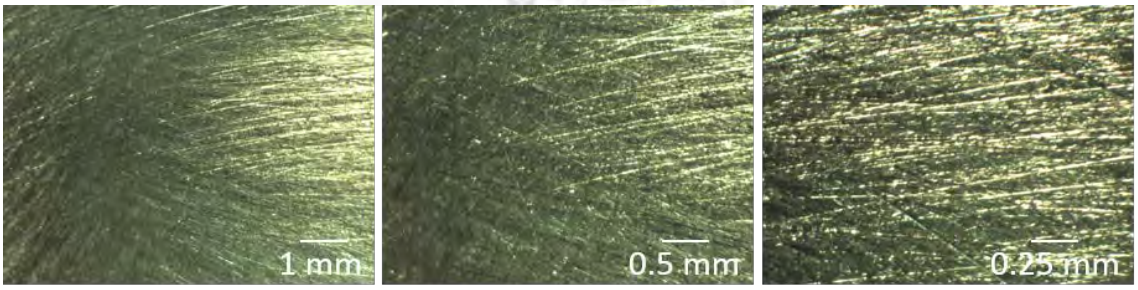

Ra (µm)	Rq (µm)	Rz (µm)	Rs (mm)
.0512	.638	2.867	.0079
.535	.686	3.234	.0078

Finish: Ground Surface

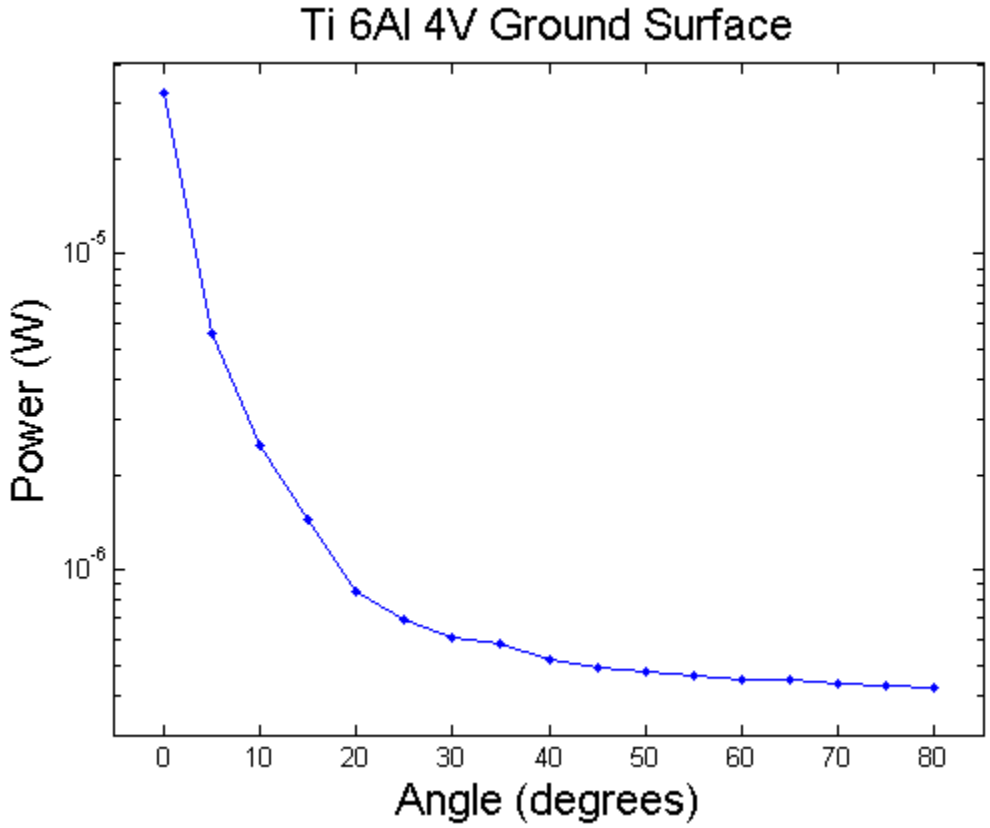

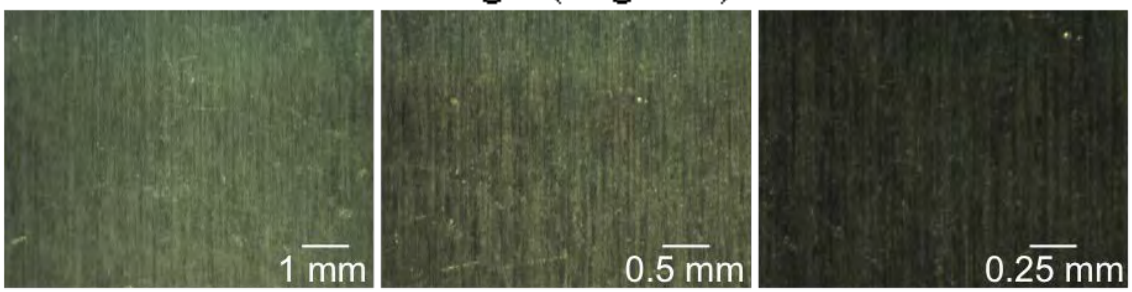

Ra (µm)	Rq (µm)	Rz (µm)	Rs (mm)
.830	1.050	3.585	.0188
.591	.812	3.515	.0171

Appendix D. Mg AZ31B Reflected Power Measurements as a Function of Angle, Surface Profilometery, and Optical Photography at 10-, 20-, and 40-Times Magnifications

This appendix appears in its original form, without editorial change.

Surface profilometry of Mg AZ31B was acquired at two spots because of the significant texture variation across the surface, one that was deemed relatively rough as assessed by eye and one that was deemed relatively smooth as assessed by eye.

Finish: As-is

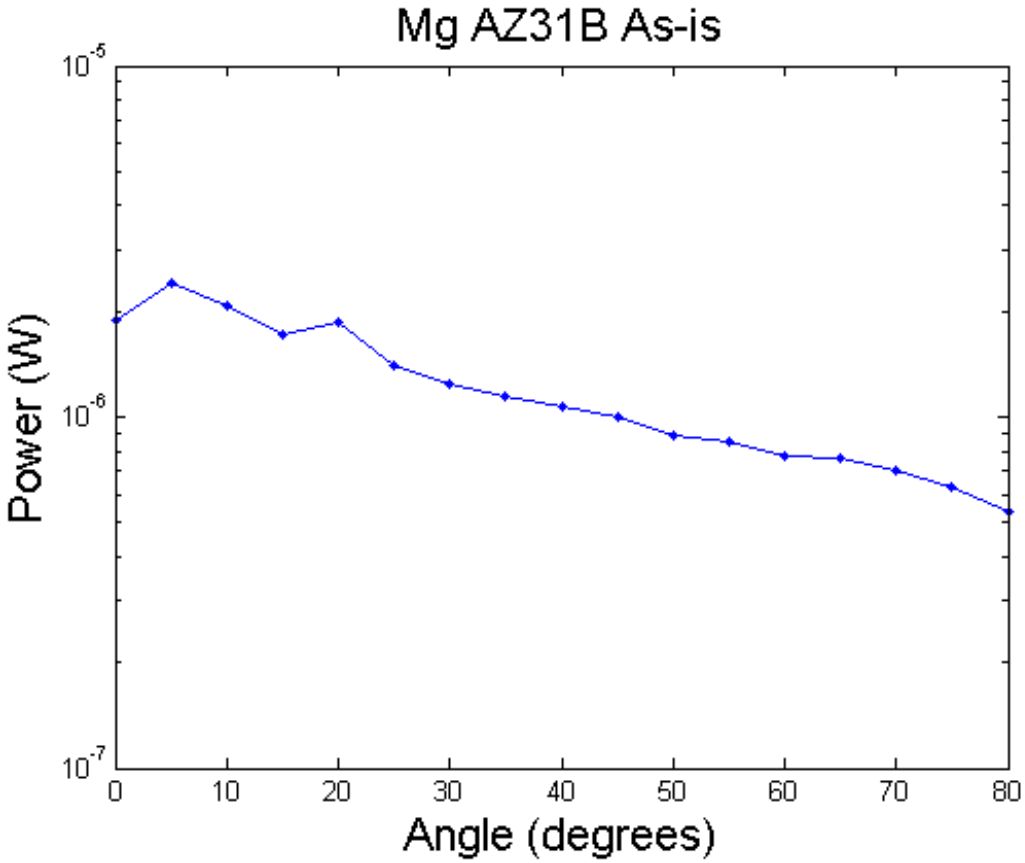

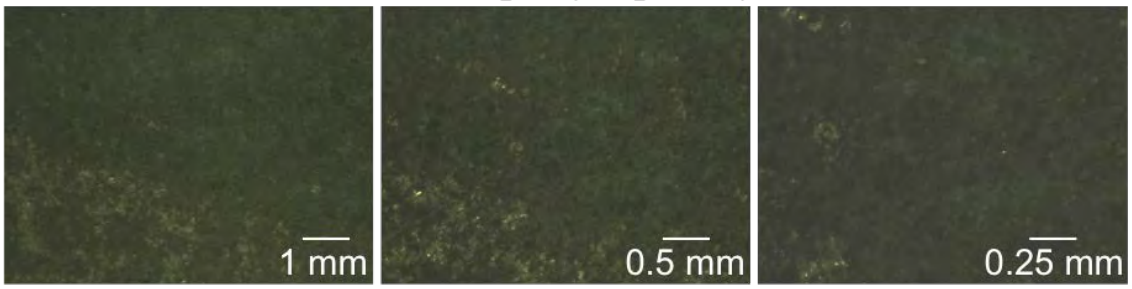

Ra (µm)	Rq (µm)	Rz (µm)	Rs (mm)
1.248	1.724	5.554	.0425
1.005	1.342	5.773	.0404

Finish: Machined (Fly Cutter)

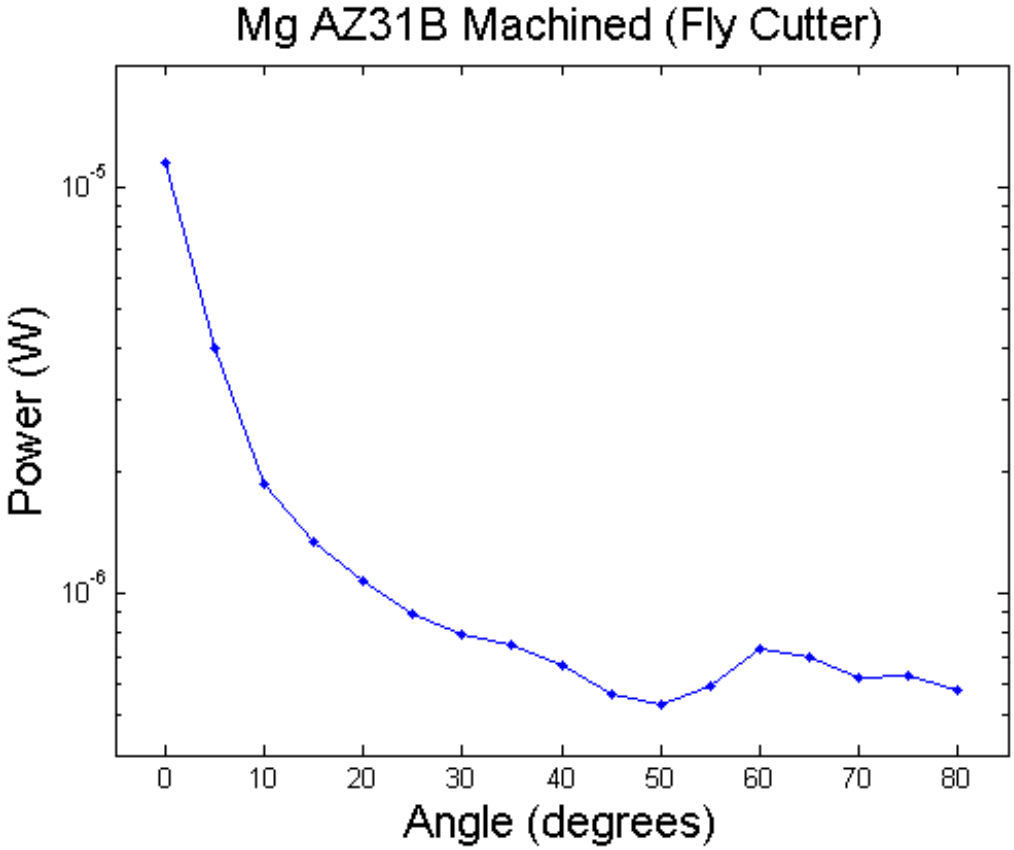

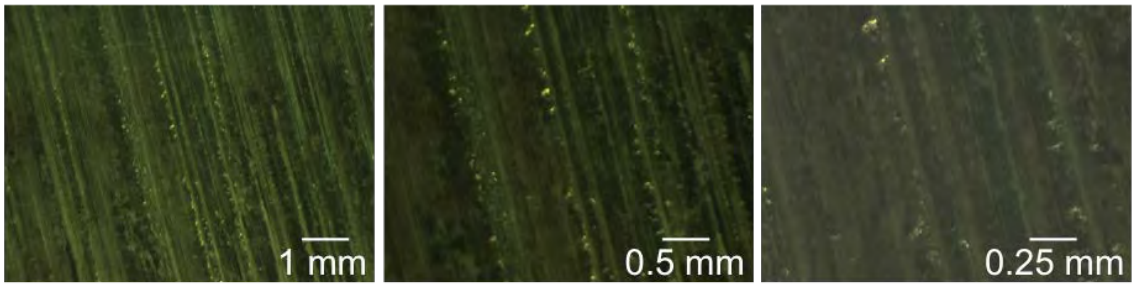

Ra (µm)	Rq (µm)	Rz (µm)	Rs (mm)
0.698	.860	2.914	.0367
.790	.912	2.96	.0065

Finish: Sandblasted

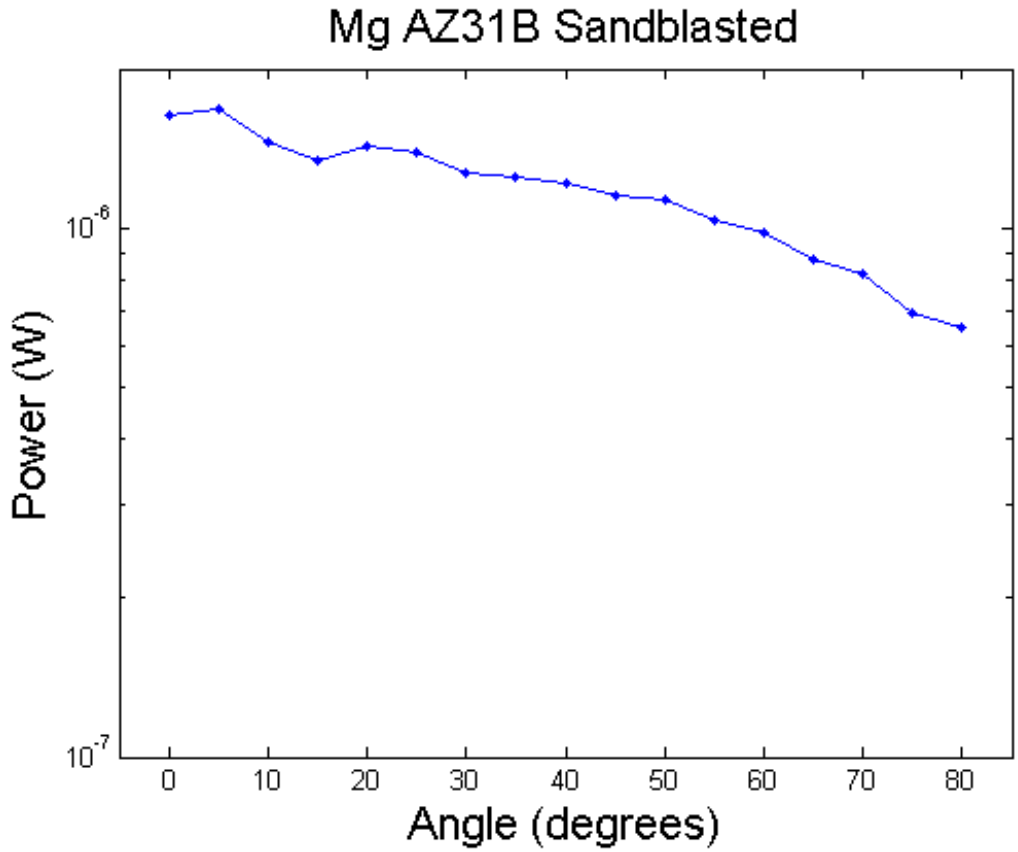

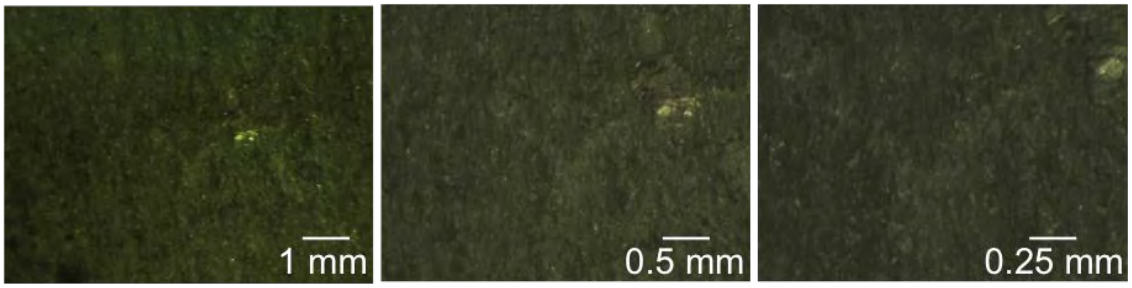

Ra (µm)	Rq (µm)	Rz (µm)	Rs (mm)
4.768	6.039	18.33	.0493
5.714	7.512	22.0	.0451

Finish: Sanded

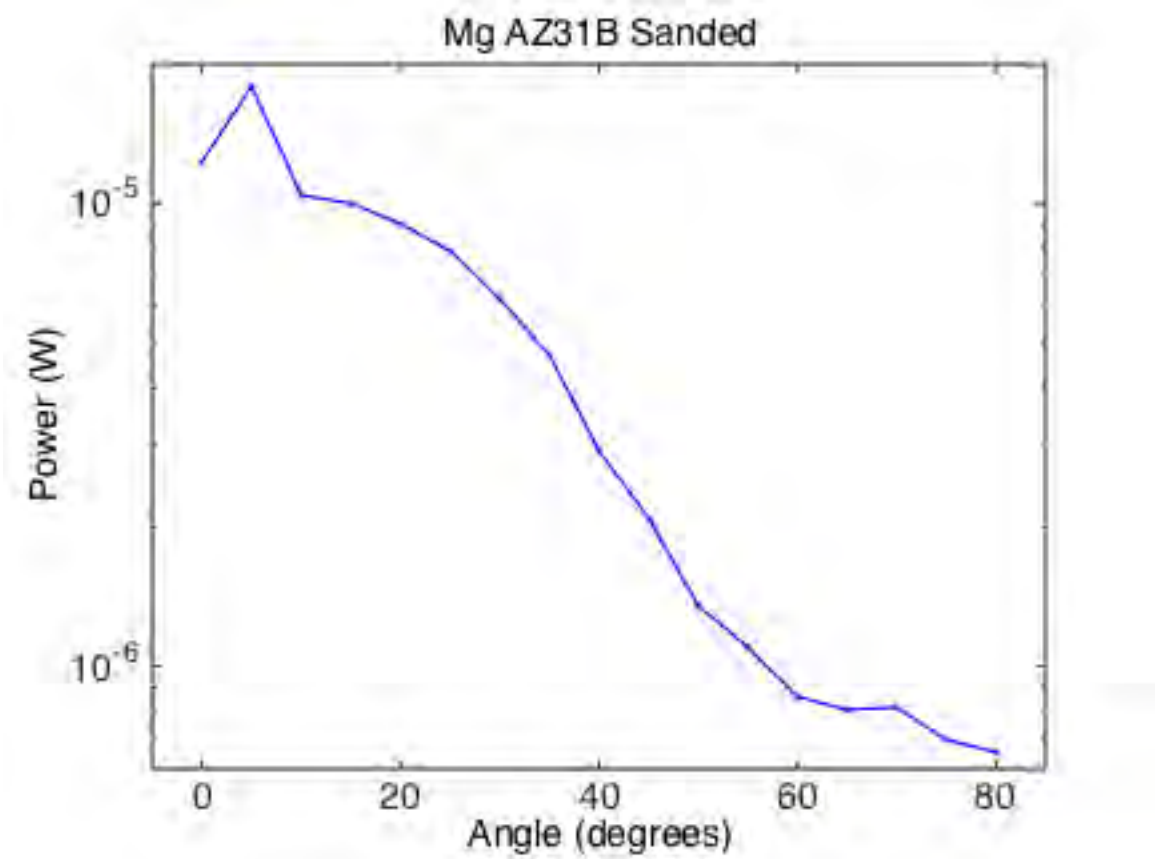

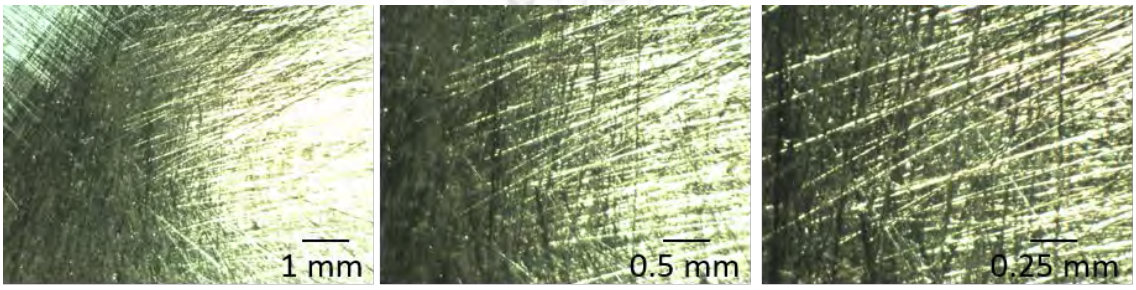

Ra (µm)	Rq (µm)	Rz (µm)	Rs (mm)
1.017	1.267	5.484	.0252
.975	1.253	5.992	.0238

Finish: Ground Surface

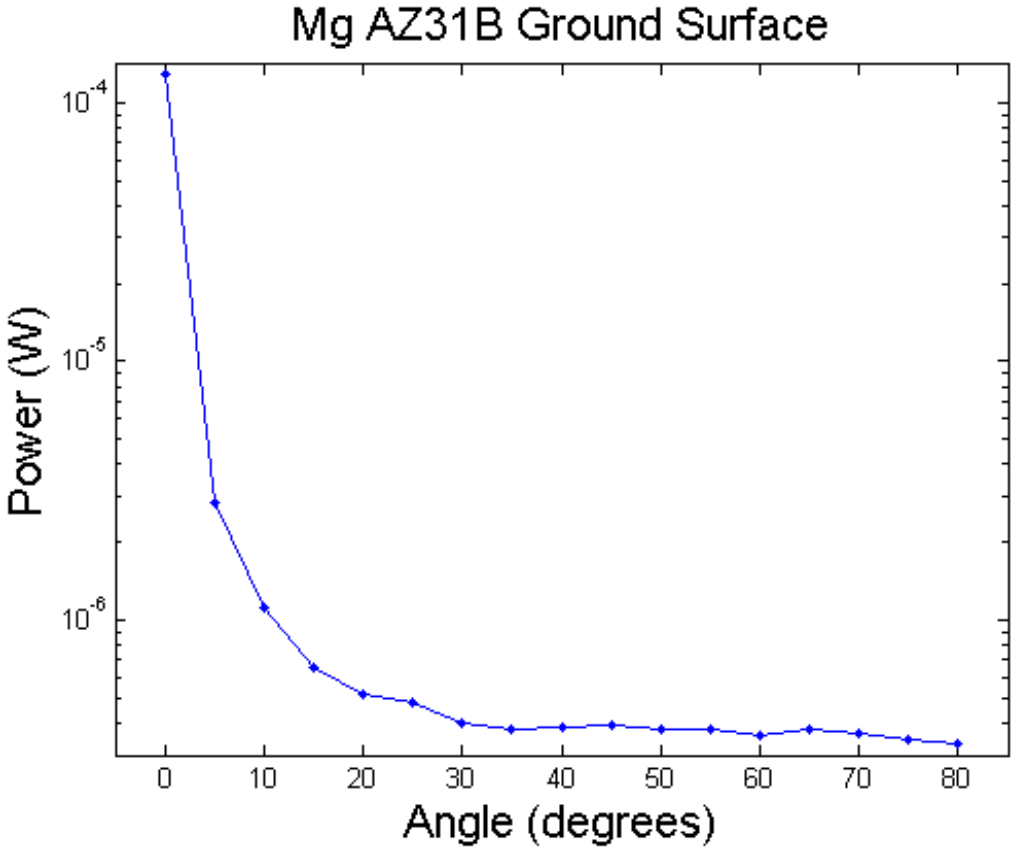

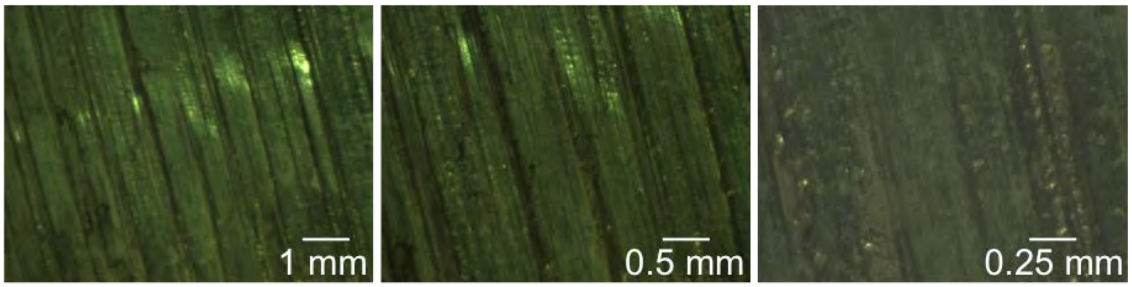

Ra (µm)	Rq (µm)	Rz (µm)	Rs (mm)
0.505	0.623	2.437	.0068
.379	.532	1.554	.0174

Appendix E. Helmet Reflected Power Measurements as a Function of Angle, Surface Profilometery, and Optical Photography at 10-, 20-, and 40-Times Magnifications

This appendix appears in its original form, without editorial change.

Finish: Inside As-is

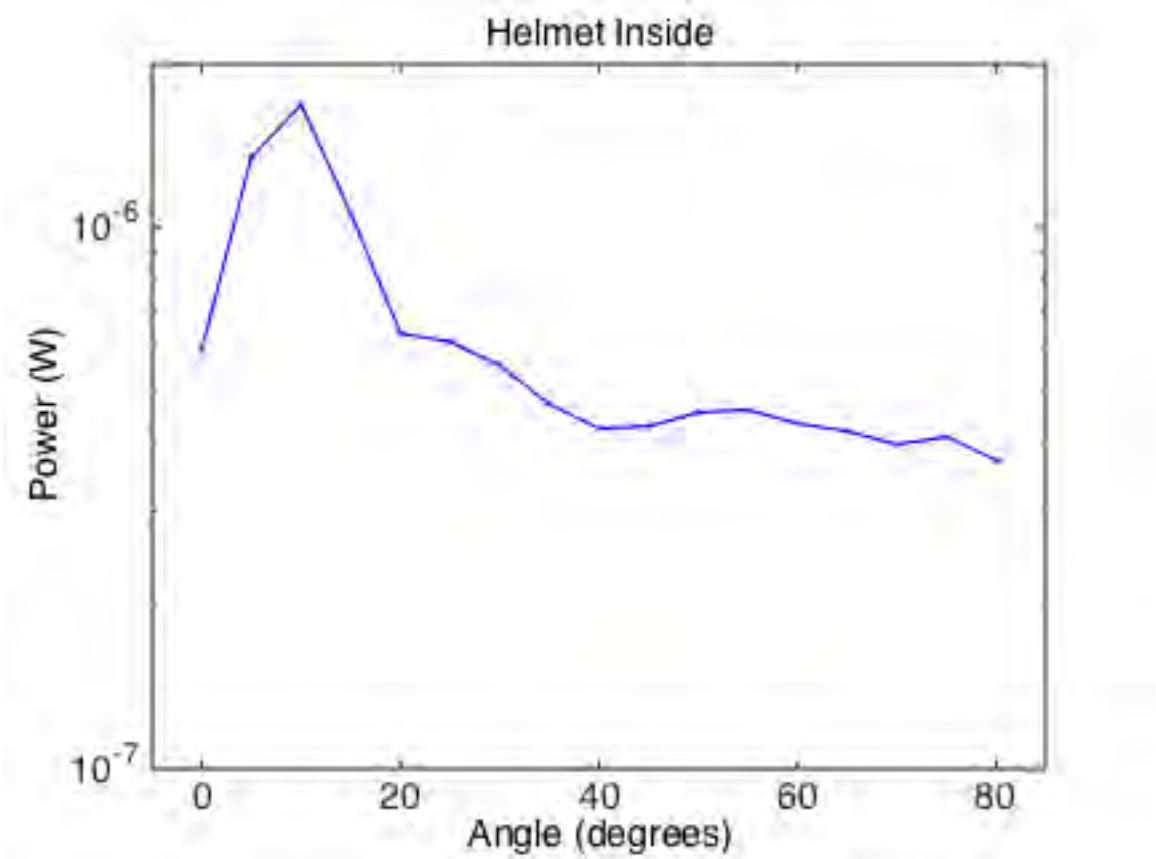

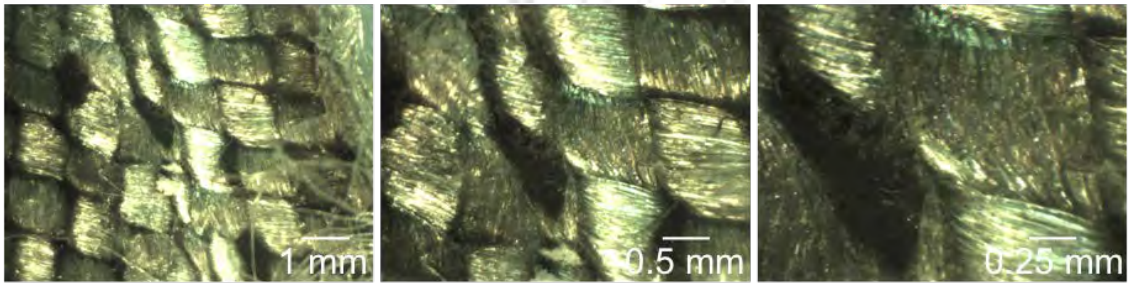

Ra (µm)	Rq (µm)	Rz (µm)	Rs (µm)
3.476	4.355	12.09	.0540

Finish: Outside As-is (painted)

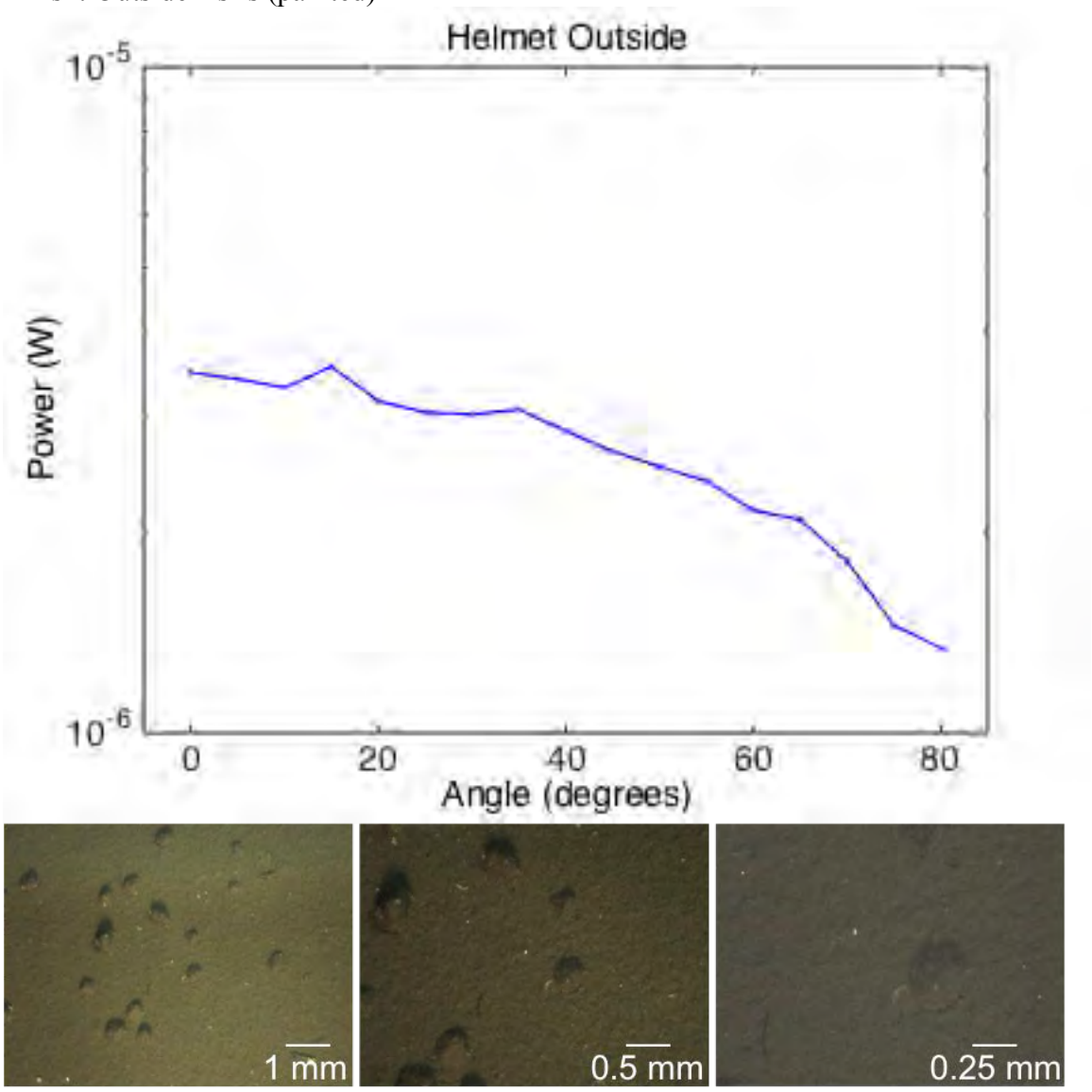

Ra (µm)	Rq (µm)	Rz (µm)	Rs (mm)
3.751	4.675	18.08	.0267

INTENTIONALLY LEFT BLANK.

Appendix F. Spectra Shield II Reflected Power Measurements as a Function of Angle, Surface Profilometery, and Optical Photography at 10-, 20-, and 40-Times Magnifications

This appendix appears in its original form, without editorial change.

Finish: As-is (pressed)

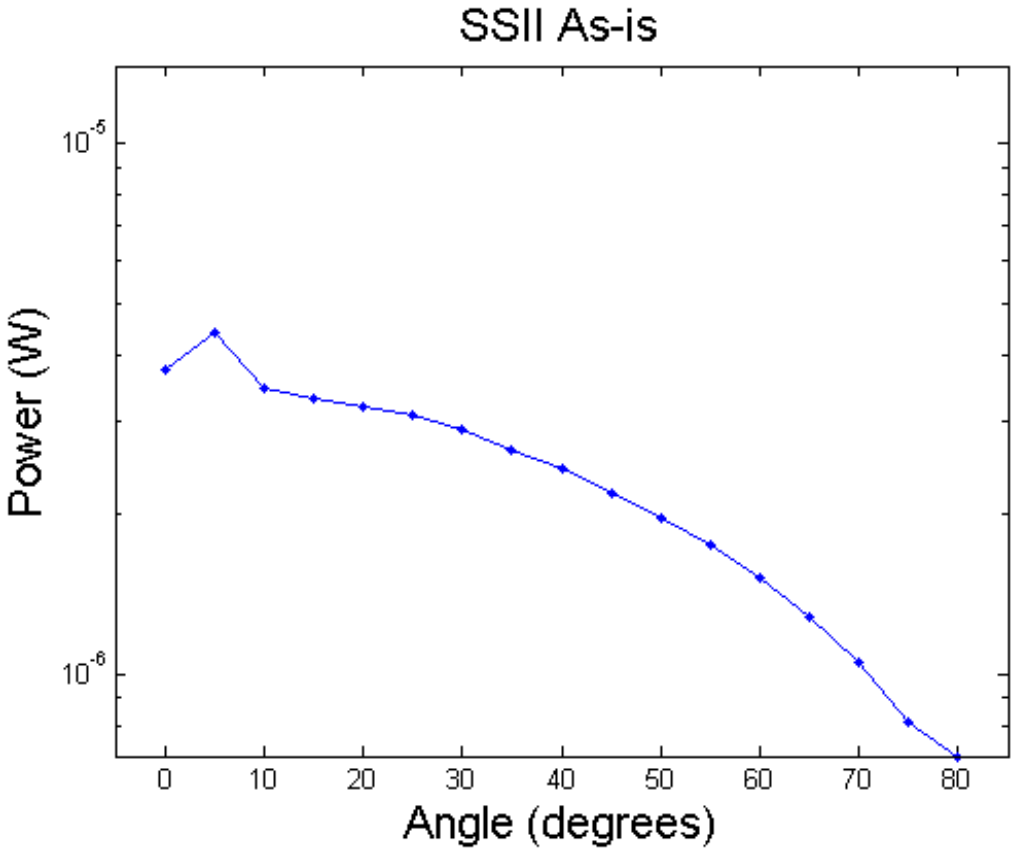

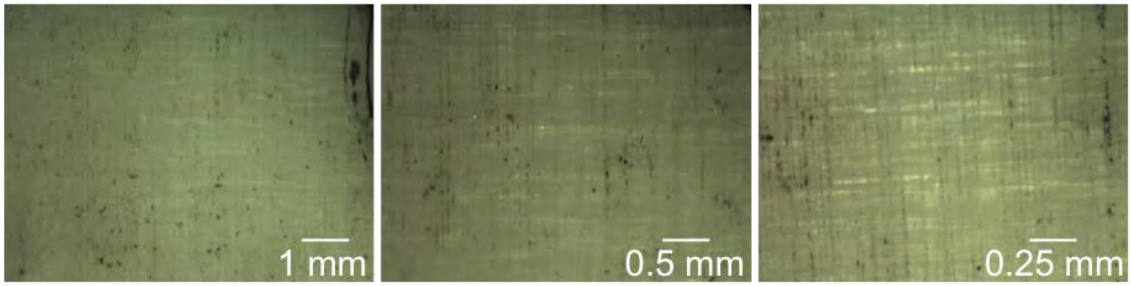

Ra (µm)	Rq (µm)	Rz (µm)	Rs (mm)
1.880	2.359	10.04	.0313

Finish: Saw Cut

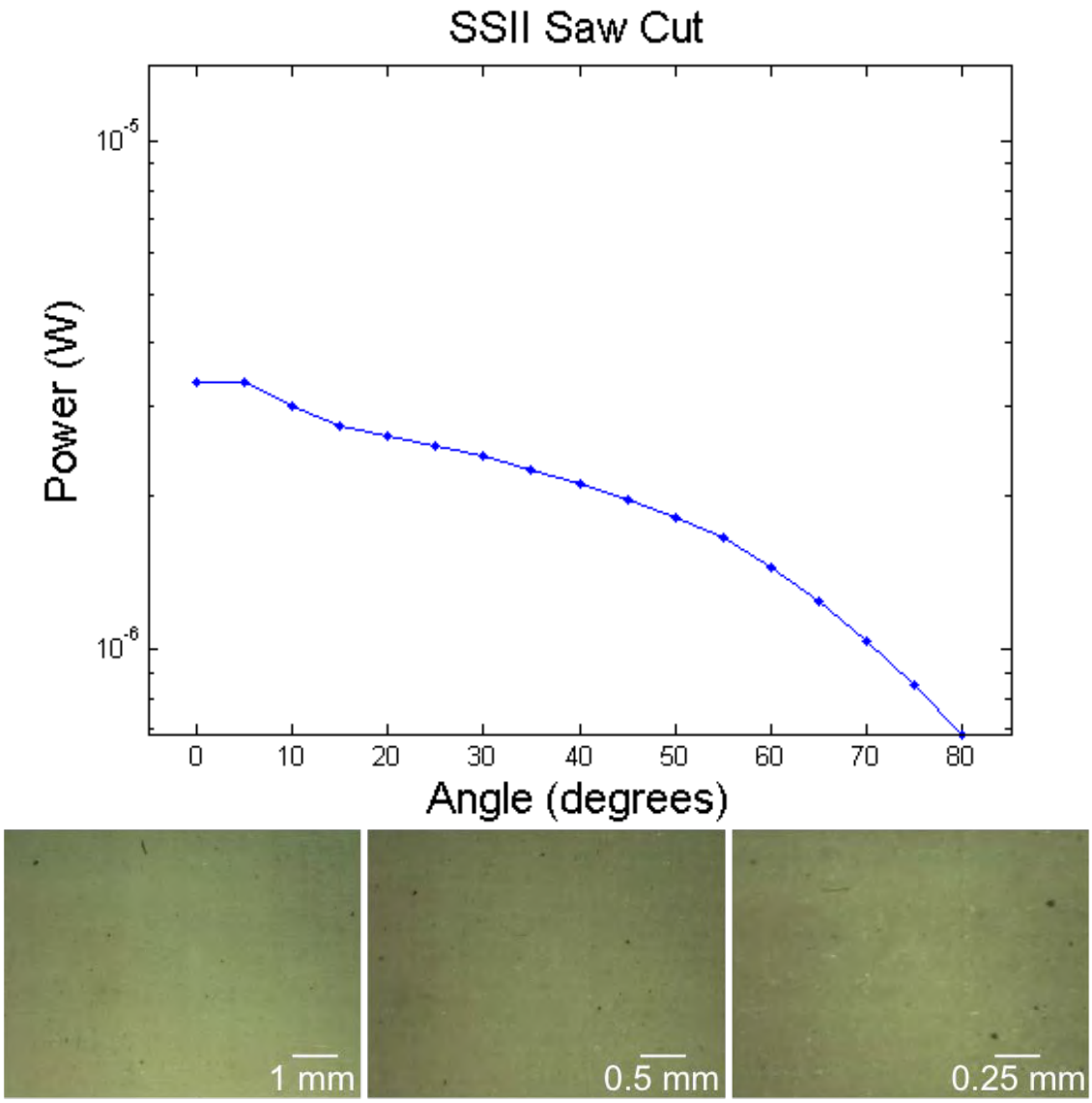

Ra (µm)	Rq (µm)	Rz (µm)	Rs (mm)
3.470	4.229	10.89	.0727

Finish: Waterjet Cut

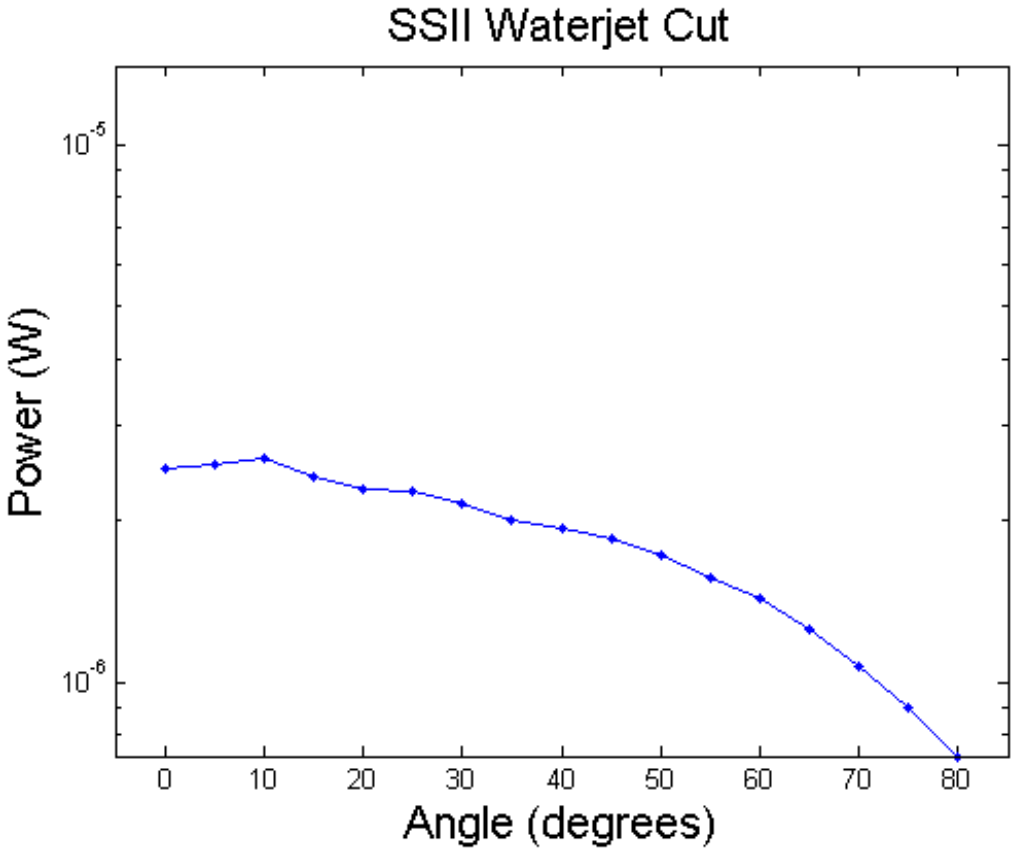

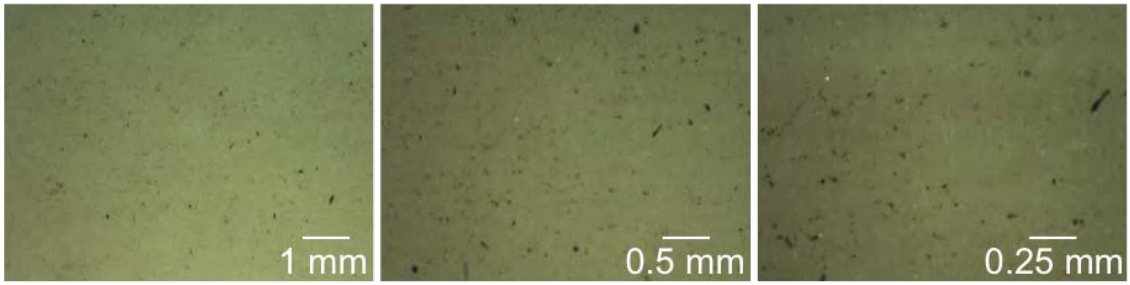

Ra (µm)	Rq (µm)	Rz (µm)	Rs (mm)
3.864	4.770	12.00	.0678

Appendix G. Dyneema HB-26 Reflected Power Measurements as a Function of Angle, Surface Profilometery, and Optical Photography at 10-, 20-, and 40-Times Magnifications

This appendix appears in its original form, without editorial change.

Finish: As-is (pressed)

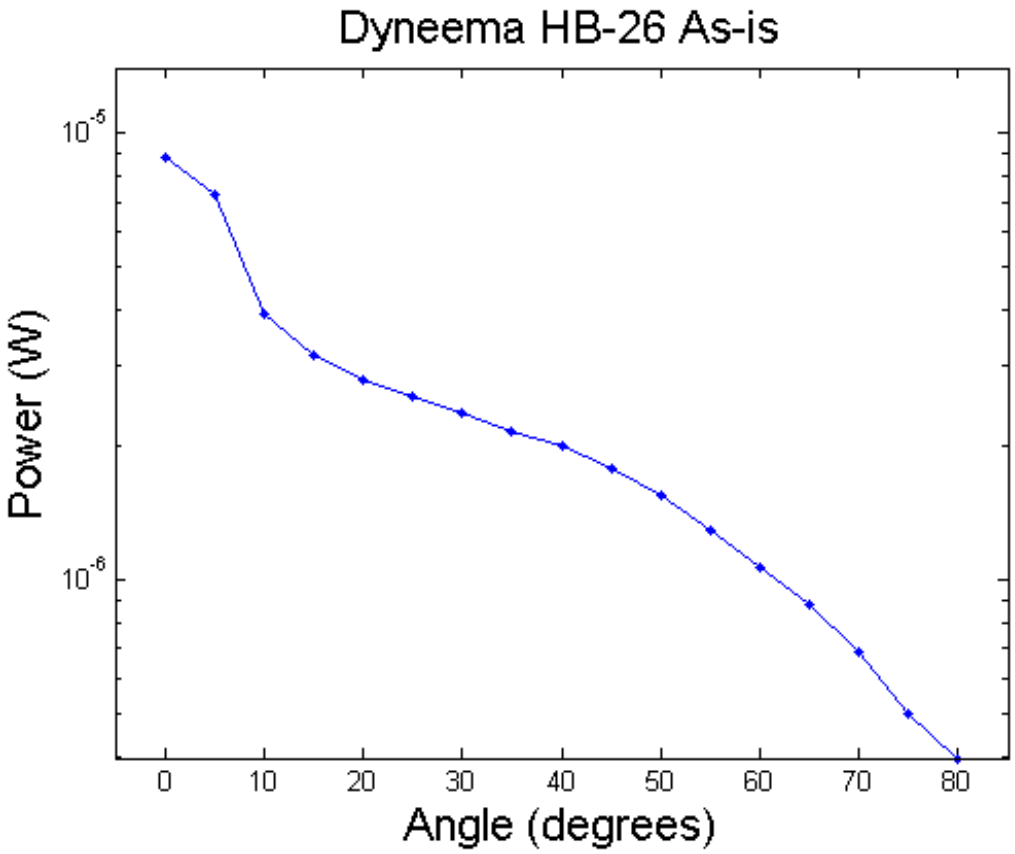

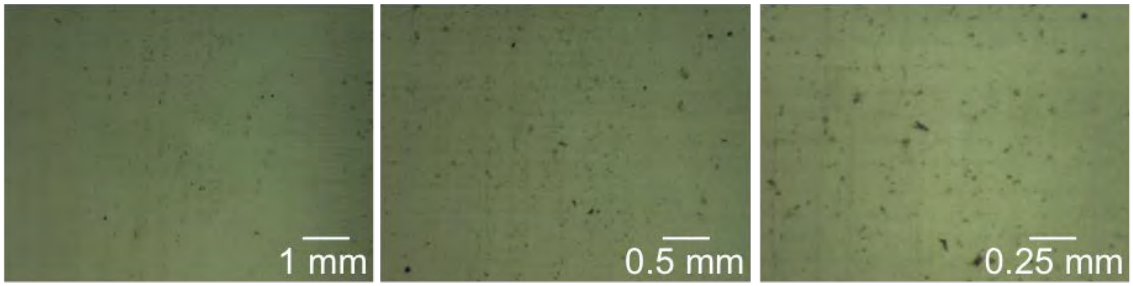

Ra (µm)	Rq (µm)	Rz (µm)	Rs (mm)
1.871	2.264	7.562	.0843

Finish: Saw Cut

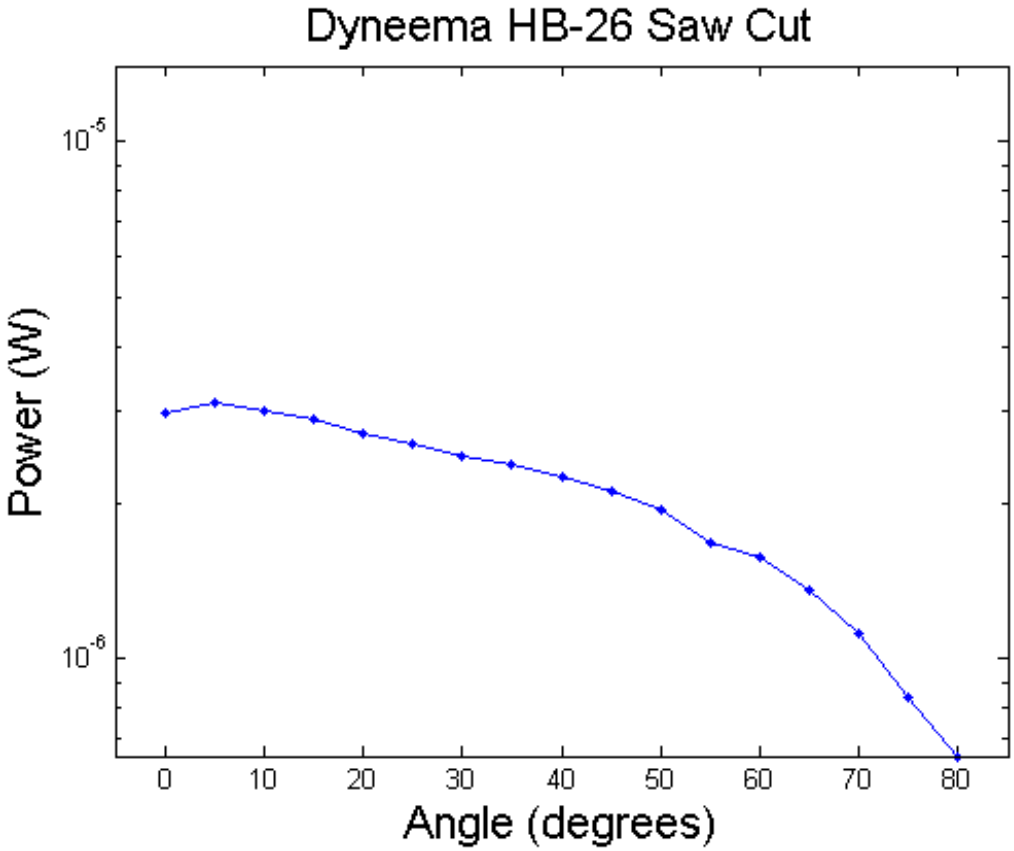

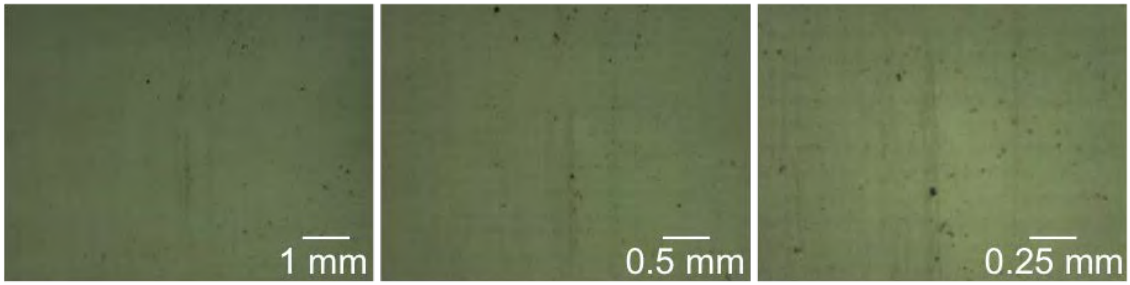

Ra (µm)	Rq (µm)	Rz (µm)	Rs (mm)
2.051	2.667	12.29	.0553

Finish: Waterjet Cut

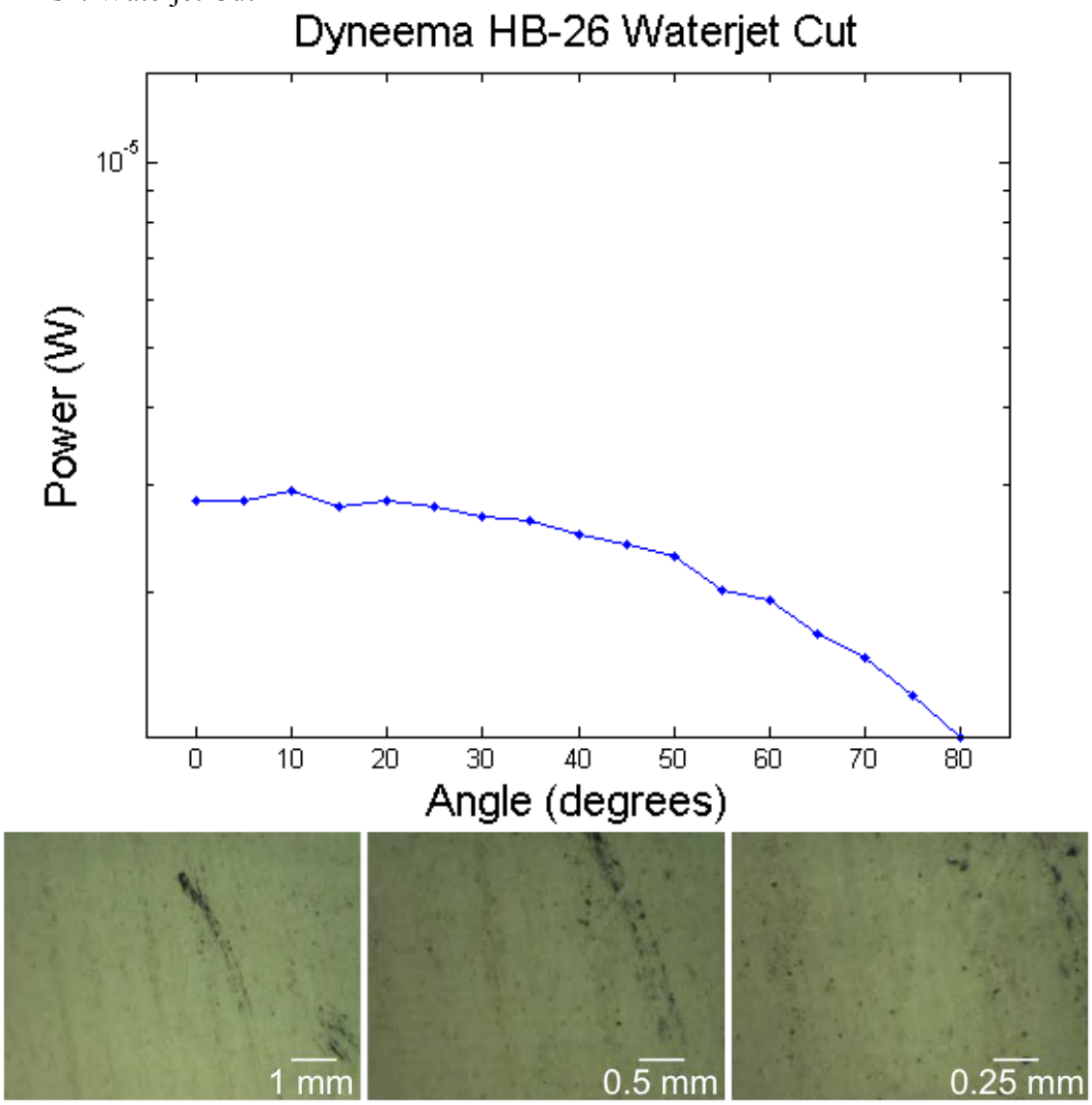

Ra (µm)	Rq (µm)	Rz (µm)	Rs (mm)
4.168	4.842	11.20	.0379

Appendix H. Al_2O_3 Reflected Power Measurements as a Function of Angle, Surface Profilometery, and Optical Photography at 10-, 20-, and 40-Times Magnifications

This appendix appears in its original form, without editorial change.

Finish: As-is

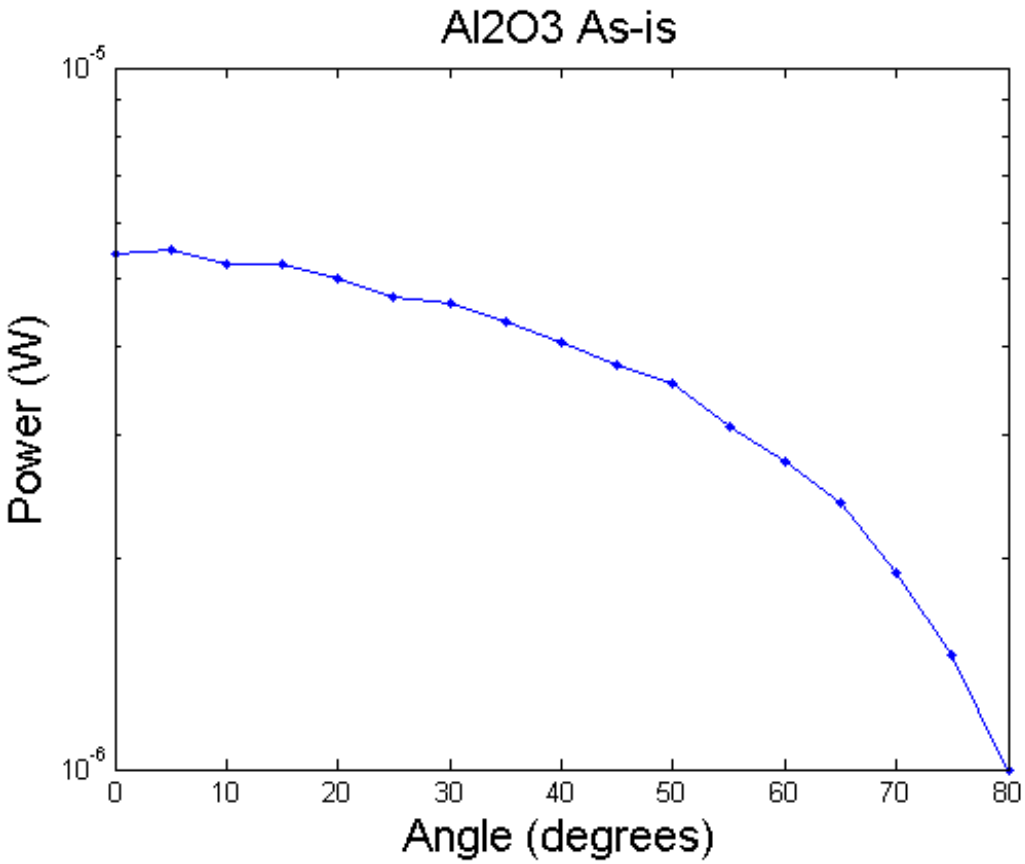

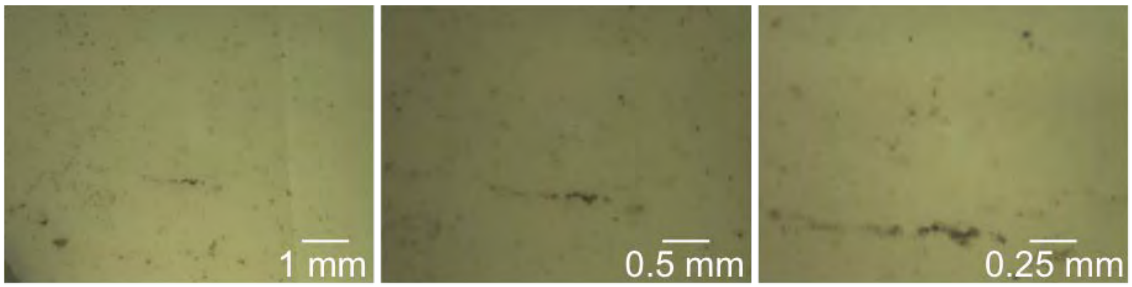

Ra (µm)	Rq (µm)	Rz (µm)	Rs (mm)
0.856	1.093	4.312	.0183

Appendix I. Polyethylene Reflected Power Measurements as a Function of Angle, Surface Profilometery, and Optical Photography at 10-, 20-, and 40-Times Magnifications

This appendix appears in its original form, without editorial change.

Finish: As-is (extruded)

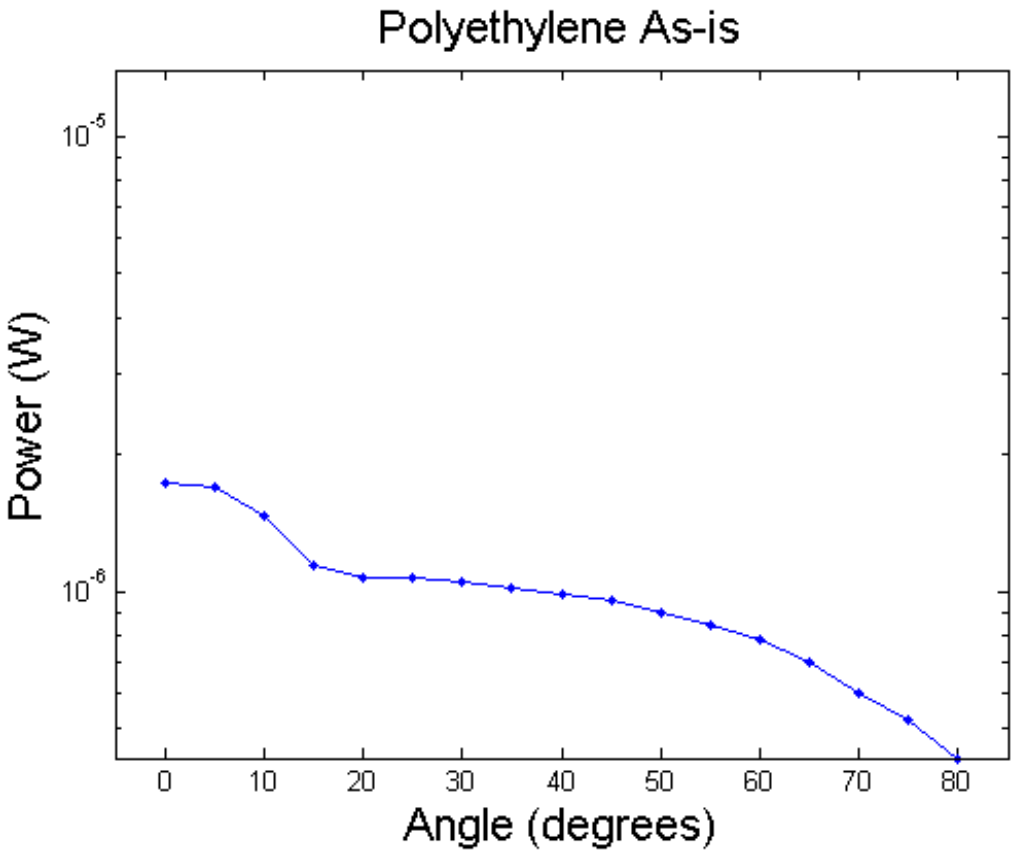

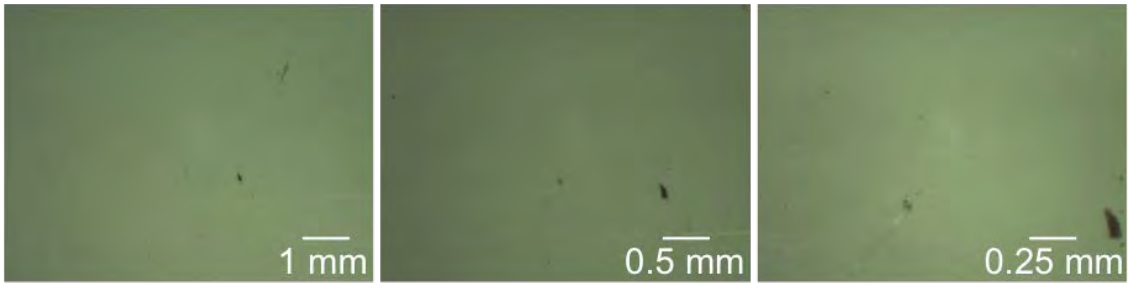

Ra (µm)	Rq (µm)	Rz (µm)	Rs (mm)
0.293	0.502	2.828	.1508

Finish: Saw Cut

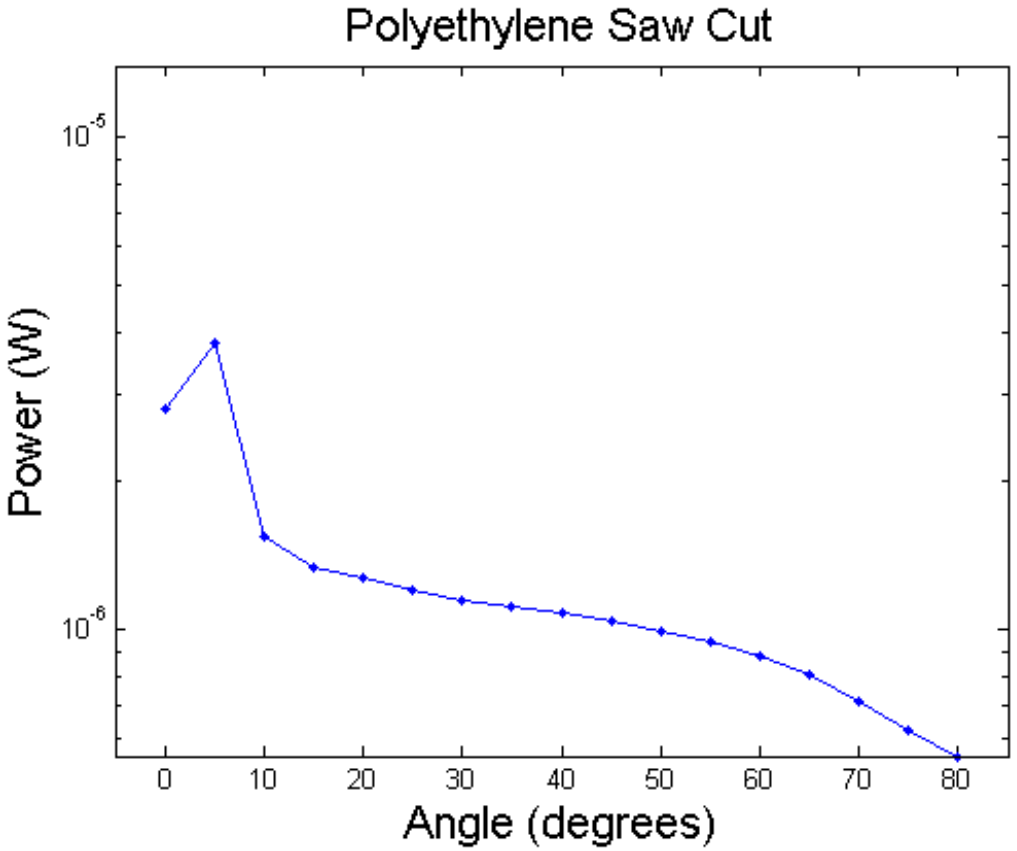

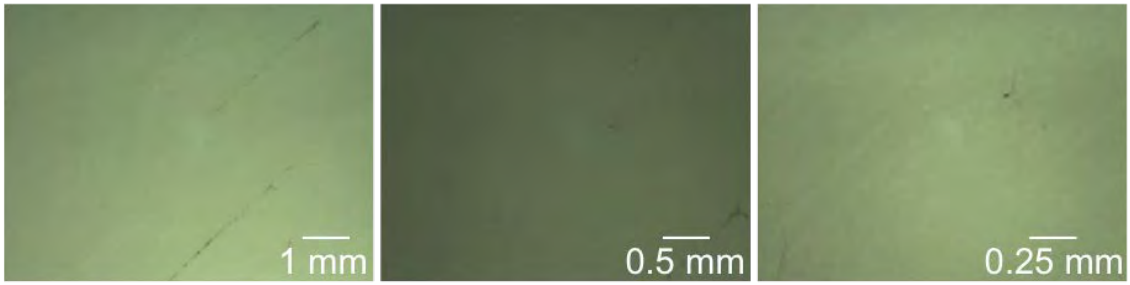

Ra (µm)	Rq (µm)	Rz (µm)	Rs (mm)
9.493	11.68	35.21	.1328

INTENTIONALLY LEFT BLANK.

Appendix J. Kevlar Reflected Power Measurements as a Function of Angle, Surface Profilometery, and Optical Photography at 10-, 20-, and 40-Times Magnifications

This appendix appears in its original form, without editorial change.

Finish: As-is (pressed)

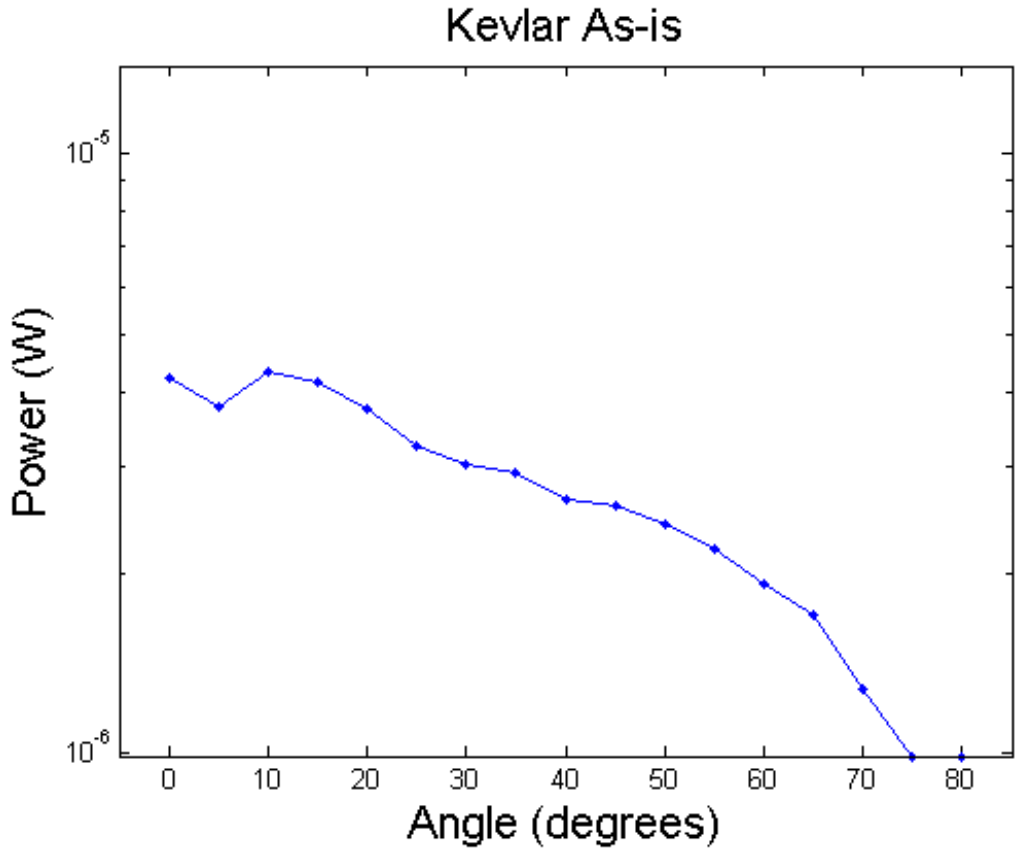

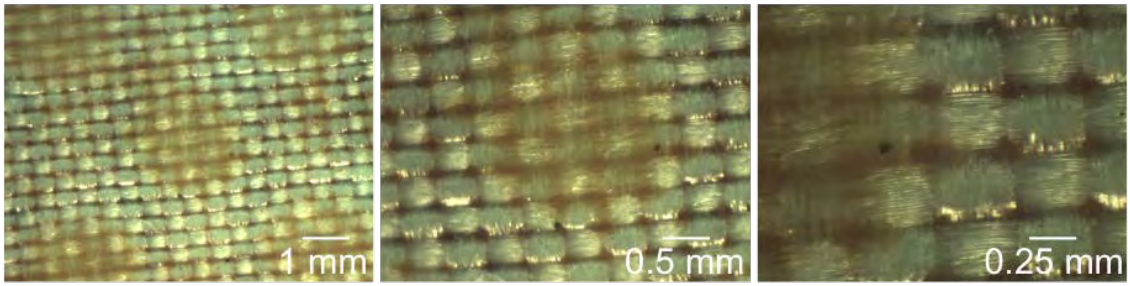

Ra (µm)	Rq (µm)	Rz (µm)	Rs (mm)
8.057	9.812	35.28	.0807

Finish: Waterjet Cut

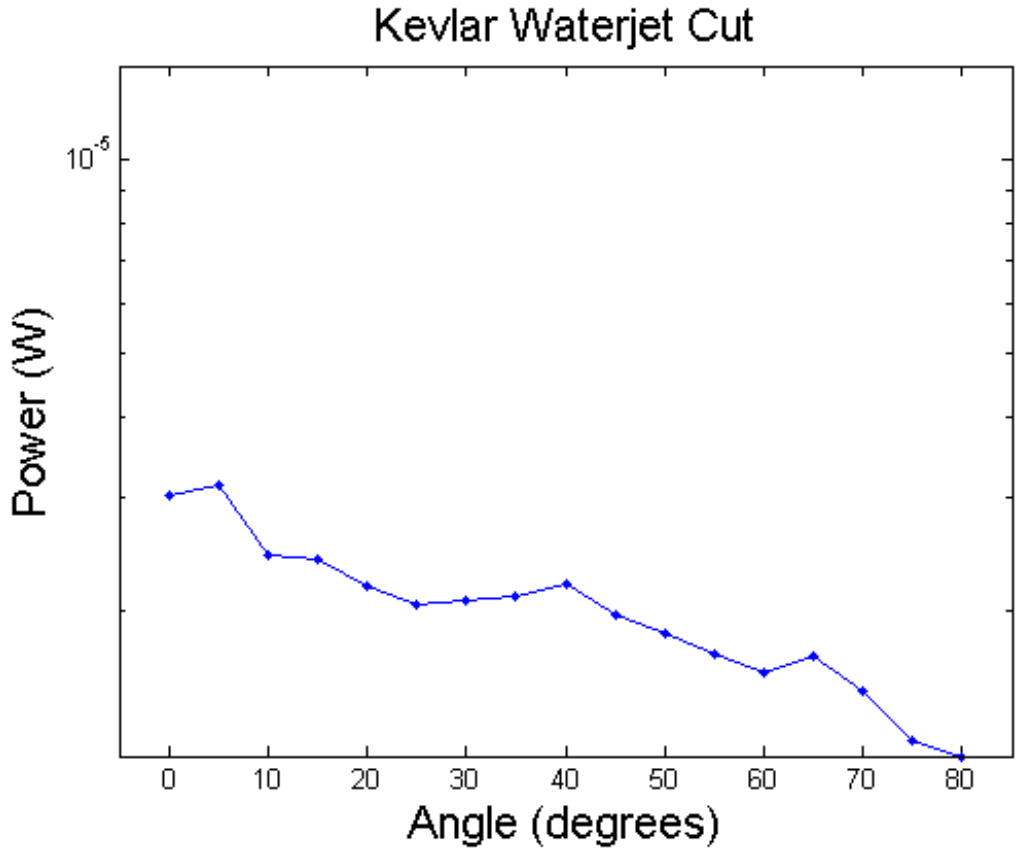

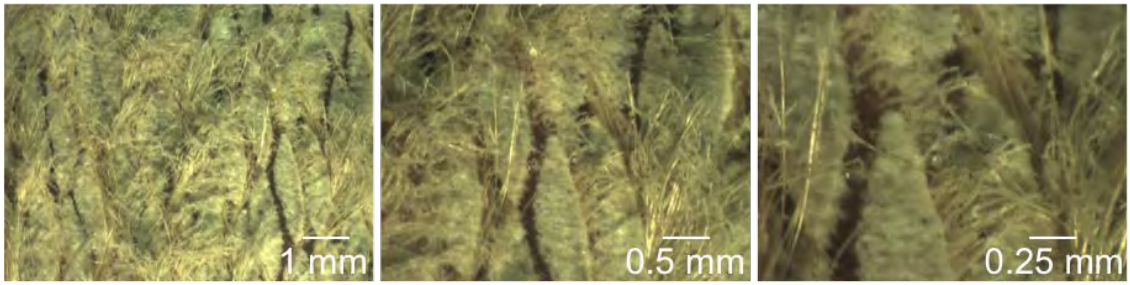

Ra (µm)	Rq (µm)	Rz (µm)	Rs (mm)
NA	NA	NA	NA

INTENTIONALLY LEFT BLANK.

Appendix K. Mild Steel Reflected Power Measurements as a Function of Angle, Surface Profilometery, and Optical Photography at 10-, 20-, and 40-Times Magnifications

This appendix appears in its original form, without editorial change.

Finish: Cut (Lathe)

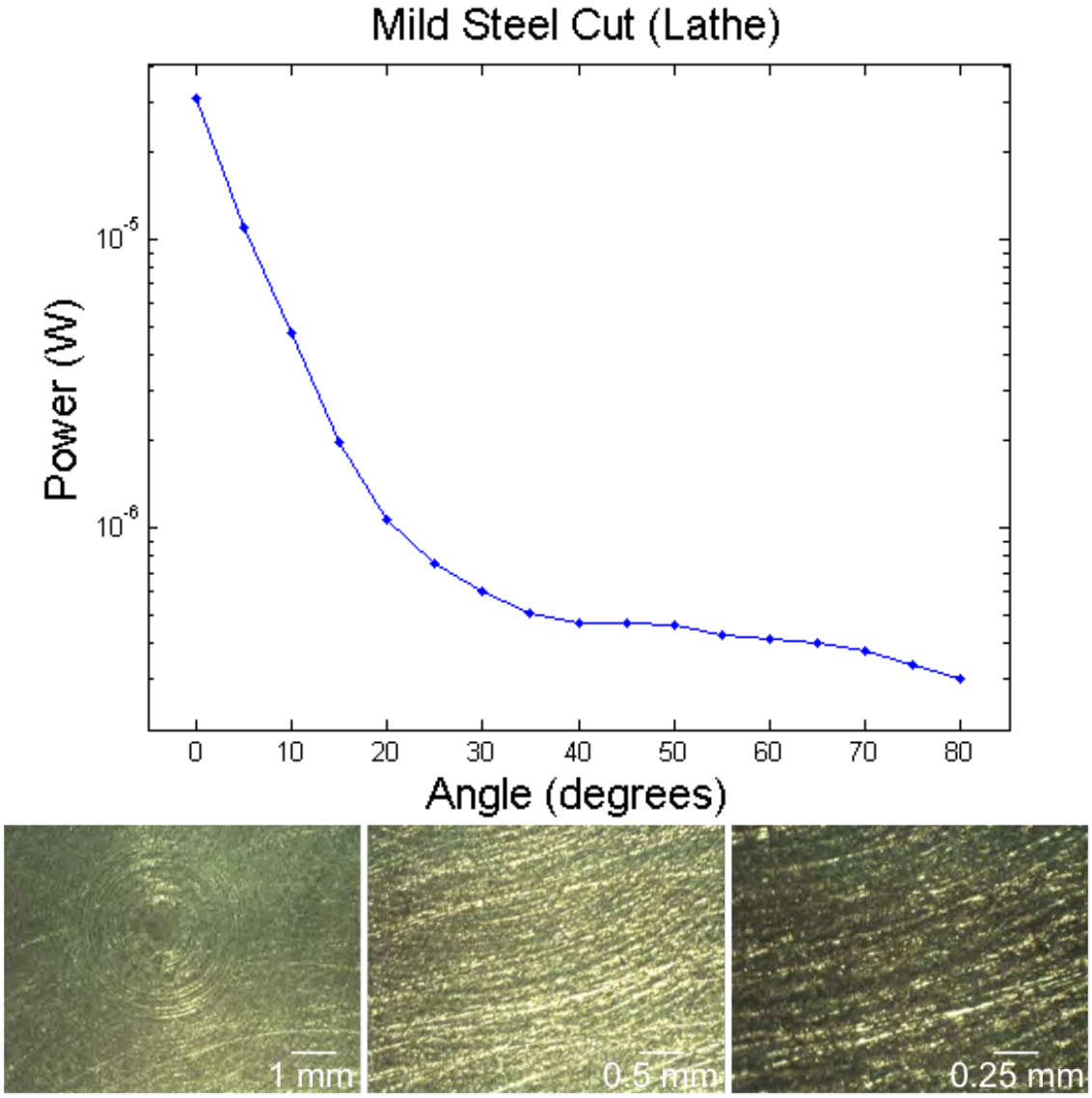

Ra (µm)	Rq (µm)	Rz (µm)	Rs (mm)
0.856	1.025	3.117	.0284

1 (PDF)	DEFENSE TECHNICAL INFORMATION CTR DTIC OCA
2 (PDF)	DIRECTOR US ARMY RESEARCH LAB RDRL CIO LL IMAL HRA MAIL & RECORDS MGMT
1 (PDF)	GOVT PRINTG OFC A MALHOTRA
15 (PDF)	DIR USARL RDRL WML H B SCHUSTER RDRL WMP D A BARD R DONEY M KEELE D KLEPONIS H MEYER F MURPHY J RUNYEON M ZELLNER B SCOTT G VUNNI S SCHRAML RDRL WMP B B LEAVY RDRL WMP E P SWOBODA K DUDECK

INTENTIONALLY LEFT BLANK.